

# Renewable origin, additionality, temporal and geographical correlation – eFuels production in Germany under the RED II regime

Uwe Langenmayr<sup>\*</sup>, Manuel Ruppert

*Institute for Industrial Production, Karlsruhe Institute of Technology, Karlsruhe, Germany*

## ARTICLE INFO

### Keywords:

eFuels  
Renewable energy directive  
Energy system analysis  
Hydrogen  
Synthesis

## ABSTRACT

E-fuels are a promising technological option to reduce the carbon footprint in the transportation sector. To ensure the renewable origin of electricity-based fuels and minimize the impact of power-to-liquid facilities on the electricity grid, the European Union implemented electricity purchase conditions within the Renewable Energy Directive II. In this work, we analyze the impact of these electricity purchase conditions on the optimal placement, dimensioning and operation of facilities and the German electricity system. The results show that implementing the proposed electricity purchase conditions increases electrolysis capacity by 15.8% and reduces utilization by 672 h in 2030. With the constrained electricity supply, the power-to-liquid facilities concentrate on network nodes with high renewable potential, while the carbon dioxide supply loses importance. Overall, the German electricity system is not heavily affected by the proposed purchase conditions as the required renewable generation capacities only increase slightly. At the same time, carbon dioxide abatement costs rise by 14.3% by introducing the electricity purchase conditions.

## 1. Introduction

While the transition of the European electricity sector towards a lower carbon footprint is in full swing, changes in the industry, heat and transportation sectors are materializing at a much slower pace. In the transportation sector, rising transport volume and the increasing weight of passenger cars have led to growing greenhouse gas (GHG) emissions in recent years. Consequently, the European Union aims to increase the speed of transformation of the different sectors. The primary legislative implementation is the Renewable Energy Directive 2018/2001 (RED II) (European Union, 2022), which introduces a minimum share of renewable energies in final energy consumption within the transport sector of 14% by 2030. Germany aims to surpass this target and plans to achieve at least 28% renewable share within the same timeframe.

Electricity-based synthetic fuels (eFuels) are one viable technology that enables lower or even zero emissions for combustion-based mobility. Hydrogen is one of the starting products in the eFuels production process and is based on the electrolysis process, where water is split into hydrogen and oxygen using electricity. Hydrogen itself can be considered an eFuel, but it can also be processed into carbon-based eFuels for transportation like gasoline, diesel and kerosene. Here, carbon dioxide (CO<sub>2</sub>) is obtained from local sources via CO<sub>2</sub> scrubbing or

from the atmosphere via direct air capture (DAC). Different synthesis processes exist to convert the synthetic gas to eFuels, for example, the Fischer-Tropsch (FTS) process and the methanol-to-gasoline route. As such, eFuels can be considered a complementary technology to battery-electric transportation, and can play a significant role when meeting transportation needs where battery technology is not well suited. For example, battery storage is less favorable for long-distance (e.g., international aviation) and heavy-duty transportation (e.g., shipping). This is mainly due to the battery's low energy density, which requires large and thus heavy batteries for these types of transportation (Siegemund et al., 2017). Furthermore, as the passenger car fleet will still consist of a large amount of internal combustion engine vehicles in the future due to the inertia of the fleet (Luderer et al., 2021), eFuels might be the only alternative to achieve carbon neutrality within the existing fleet.

## 2. Background on the renewable energy directive II in the context of eFuel production

The Green Deal is the central climate policy initiative to achieve carbon neutrality by 2050 in the European Union. The initiative includes a 50–55% reduction of GHG emissions by 2030 compared to the GHG emission levels of 1990. The Green Deal also includes specific policy

<sup>\*</sup> Corresponding author.

E-mail address: [uwe.langenmayr@kit.edu](mailto:uwe.langenmayr@kit.edu) (U. Langenmayr).

proposals to reduce GHG emissions and increase the renewable energy share in all sectors. The European Union's adjustment of climate objectives was followed by revisions of existing policies. One of these policies, the RED II, established a legal framework and common principles to promote the use of renewable energy sources and an efficient energy system integration in the European Union. The vision of an integrated energy system includes all sectors, aiming to increase the renewable energy share not only in the electricity sector. One aspect of RED II assesses the different technologies in the transportation sector. It describes which and how technologies can be used within the integrated energy system, if quotas or limitations exist, and how national members of the European Union can use crediting systems to assess the contribution of the different technologies to national GHG reduction.

Today, eFuel production faces complex challenges. First, additional electrical demand from hydrogen production can lead to new or increased congestion in the electricity grid, especially when electricity demand from eFuel production and renewable electricity generation are spatially remote in a generally congested transmission grid environment. Second, to ensure the renewable property of eFuels, electricity needs to stem primarily or exclusively from renewable energy sources and should not lead to higher GHG emissions than the utilization of conventional fuels.

In RED II, the European Commission proposed a catalogue of requirements in Art.27(3) to assess eFuels as renewable fuels of non-biological origin (RNFBO). On one hand, the production of eFuels with grid-independent renewable energy sources (RES) is regulated in Art.4(1). This option is especially reasonable if high potentials of RES exist and eFuel production does not collide with other renewable energy targets. On the other hand, grid-connected eFuel production is defined in Art.4(2). Here, the RNFBO status is achieved if the renewable energy share in the bidding zone is at least 90% in the last calendar year and the operation time of the electrolysis does not exceed the time with renewable generation. Alternatively, sourcing electricity from the grid is possible if the emission intensity of the electricity is lower than 18 gCO<sub>2</sub>eq/MJ.

Grid-connected eFuel production that is RNFBO-compatible is also possible in bidding zones with a lower share of renewable energy, but the requirements are more comprehensive. In the aforementioned case, the RNFBO status can be achieved by obtaining a private purchase agreement for the required amount of electricity while meeting other electricity purchase conditions. Art.4(2)(a) determines that the RES must be commissioned within the last 36 months before the commissioning of the electrolysis unit. We refer to this limitation as the additionality constraint. Art.4(2)(b) excludes all generation from RES which has received previous subsidies. The temporal correlation condition in Art.4(2)(c) specifies that for all facilities starting production before 2030 the electricity consumption of the electrolysis does not exceed the total electricity generation of the RES within the same month. From the year 2030 on, the requirement for the temporal correlation condition changes to an hourly matching requirement. Optionally, the tightening of the correlation condition can be adopted by member states even before 2030. An increase of electrolysis utilization by using electricity storage is a suitable solution considered in the proposal. Exceptions exist if the price falls below a certain level (20 €/MWh or 0.36 times the CO<sub>2</sub> certificate price in the respective hour). Finally, Art.4(2)(d) defines the geographical correlation. Electrolysis and RES generation must be located in the same bidding zone. Alternatively, generation can be sourced from either adjacent bidding zones with equal or higher day-ahead prices at times of electricity consumption or in adjacent offshore bidding zones. Art.27(3)(12) mentions that the requirements for spatial alignment of generation and electrolysis aim at avoiding increased congestion between electric sources and sinks in the transmission network. The presented electricity purchase criteria apply for all electrolysis units from January 1, 2027.

As the electricity purchase conditions target the placement of both new RES and electrolysis, they influence the resulting optimal

placement, dimensioning and operation of eFuels production facilities. In this work, we examine two aspects of the RED II implementation: The impact of the different electricity purchase conditions on the eFuels production like capacities and capacity factors of the different components, the effect of the resulting eFuels production on the energy system in regards to generation capacities and their distribution, and finally the CO<sub>2</sub> abatement costs. The structure of the paper is as follows: The second chapter covers the existing literature on sector coupling approaches, including eFuels production, and presents the contributions this study will answer. The literature chapter is followed by a description of the methodology, which consists of the energy system model, the implemented eFuels production structure and the electricity purchase conditions. The case study chapter describes the considered scenarios, CO<sub>2</sub> sources and energy system data, and the eFuels demand. The results for the German electricity system are presented and discussed in the following chapter, followed by the policy implications of our results and a conclusion.

### 3. Literature review

Studies in the field of sector coupling focus either on scales like buildings (Wang et al., 2018), cities (Dahal et al., 2018; Heinisch et al., 2021; Nevens and Roorda, 2014), single countries (Bogdanov et al., 2021; Gudmundsson et al., 2018; Gils et al., 2021; Seljom and Rosenberg, 2018; Pensini et al., 2014; Kiviluoma and Meibom, 2011; Schill and Gerbaulet, 2015; Osorio-Aravena et al., 2021) or even several countries at the same time (Brown et al., 2018; Ashfaq et al., 2017; Meibom et al., 2007; Gea-Bermúdez et al., 2021; Blanco et al., 2018b; Capros et al., 2019; Pavičević et al., 2020; Helgeson and Peter, 2020). A distinction is also possible based on modelled coupled sectors such as transportation (Brand et al., 2012; Plötz et al., 2019; Kiviluoma and Meibom, 2011; Schill and Gerbaulet, 2015; Heinisch et al., 2021; Helgeson and Peter, 2020), heating (Gudmundsson et al., 2018; Bogdanov et al., 2021; Pensini et al., 2014; Meibom et al., 2007; Ashfaq et al., 2017; Jimenez-Navarro et al., 2020), or multi-sector approaches (Bogdanov et al., 2021; Brown et al., 2018; Osorio-Aravena et al., 2021; Gea-Bermúdez et al., 2021; Gils et al., 2021; Blanco et al., 2018b; Capros et al., 2019; Pavičević et al., 2020). An exhaustive review of differences and similarities among energy system analyses including sector coupling can be found in Hansen et al. (2019), Ramsebner et al. (2021) and Hanley et al. (2018).

The analysis of the effect of eFuels production in energy systems is still relatively limited (Ramsebner et al., 2021). Blanco et al. (2018a) examined the European energy system with the TIMES energy system model to research the potential of hydrogen and power-to-liquid (PtL). The approach consisted of conducting a systematic parameter analysis with several scenarios to research the development of different hydrogen and hydrocarbon technologies in a low-carbon energy system. The study of a carbon-neutral European energy system was conducted by Capros et al. (2019) using the PRIMES model with different decarbonization scenarios. Their aim was to examine the EU 2030 climate and energy framework, the viability, sustainability and affordability of carbon-neutrality by 2050, and necessary policies to achieve the carbon neutrality objective. Mesfun et al. (2017) used the mixed-integer linear energy system BeWhere Alps to examine the ability of Power-to-Gas and PtL processes to improve the integration of intermittent renewable energy generation in the Alpine region. Quarton and Samsatli (2020) used the mixed-integer programming software Value Web Model to optimize the complete carbon capture utilization (CCU) and storage value chain, including PtL. The energy system model Balmorel was used by Gea-Bermúdez et al. (2021) to minimize the discounted system costs of Northern-central Europe to investigate the role of sector coupling in the future energy system. Helgeson and Peter (2020) developed a multi-sector model to investigate the transition of the transport sector and the necessary interaction between European countries to achieve low-carbon transportation. They included several sector-linking

components to analyze the future role of power-to-x technologies, including PtL. The above-mentioned studies implement PtL facilities without consideration of the facilities' flexibility and subsequent limitations. Generally, the flexibility of PtL facilities is low compared to that of electrolysis units (Bogdanov et al., 2021). Assuming high flexibility might result in underestimated impact on the energy system (e.g., necessity of storage, inflexible demand). For Kazakhstan (Bogdanov et al., 2021) and Chile (Osorio-Aravena et al., 2021), PtL flexibility is considered and used in a linear programming energy system model to minimize the annual costs of the energy system, including industry, heat, transportation, and power sector. Based on these results, PtL processes result in additional base load due to their inflexibility. To our knowledge, no sector-coupling model considers the impact of electricity purchase conditions or describes the operation of PtL facilities with regards to their impact on the energy system in detail.

Complementary to large-scale energy system models, a quantitative analysis of the effects of temporal correlation between hydrogen production and electricity generation to electrolysis operation was conducted by Schlund and Theile (2022). Here, a mixed-integer Markov Chain model with different interval lengths of simultaneity was applied. Similarly, Ruhнау and Schiele (2022) analyzed a wind-hydrogen system and optimized the investment and operation under different regulations. The results showed that strict regulations will result in large over-investments to increase electrolysis utilization and might slow down the green hydrogen deployment. Both approaches investigated green hydrogen production on a single unit scale and did not give consideration to large energy system models.

Next to sector coupling models, qualitative analyses of electricity purchase conditions have already been conducted based on the example of the RED II directive. Scheelhaase et al. (2019) state that the development, production and use of eFuels for aviation need a regulatory framework to reduce the uncertainty of investors. Such regulations have not been implemented and RED II might be the basis for the implementation of national laws. Chiaramonti and Goumas (2019) qualitatively analyzed RED II regarding its impact on renewable fuels including advanced biofuels, recycled carbon fuels and RFNBOs. They state that RED II is not technology-neutral towards eFuels compared to electric mobility. In comparison, eFuels can be refused by EU member states or might have constraining electricity purchase conditions like the additionality or the temporal correlation with the electricity generation. They conclude that the current framework does not provide a sufficient investment environment for eFuels and that the development of future regulations will delay large-scale eFuel production.

In existing literature, no studies consider both eFuels production on an energy system level and the associated legislative implementation. On one hand, studies focusing on sector coupling including PtL do not consider the regulations of eFuels production. Their results lack a detailed representation of the actual operation of PtL facilities and their impact on the energy system. Other quantitative studies focus on single electrolysis units and their optimal individual operation, without considering the energy system integration in the context of sector coupling. On the other hand, the impact of RED II has been investigated by qualitative studies so far without any quantitative assessments. In this work, we contribute to existing research, as we present a set of feasible constraints that enables the implementation of electricity purchase conditions into an energy system model.

#### 4. Methodology

PyPSA parameter and variables		
Parameter/ variable	Unit	Description
$i, j$		Bus labels
$u$		Individual unit label for each generator and storage unit

(continued on next column)

(continued)

PyPSA parameter and variables		
Parameter/ variable	Unit	Description
$y$		Installation year of unit
$l$		Branch labels
$t$		Snapshot /time step labels
$\omega_t$	h	Weighting of snapshot $t$ in objective function
$g_{u,i,y,t}$	MW	Dispatch of unit
$C_{u,i,y}$	MW	Capacity of generator
$\bar{g}_{u,i,y,t}$		Availability per unit of generator capacity
$\eta_{u,i,y}$		Efficiency of unit
$r_{u,i,y}$	1/h	Generator ramp up limit per unit of capacity
$r_{d,u,i,y}$	1/h	Generator ramp down limit per unit of capacity
$c_{u,i,y}^{fix}$	€/MW	Fixed costs
$c_{u,i,y}^{var}$	€/MWh	Variable cost
$e_{u,i,y,t}$	MWh	Storage state of charge (energy level)
$E_{u,i,y}$	MWh	Storage energy capacity
$g_{u,i,y,t}^{in}$	MW	Inflow of storage unit
$g_{u,i,y,t}^{spill}$	MW	Spillage of storage unit
$d_{i,t}$	MW	Electricity demand
$f_{l,t}$	MW	Branch active power flow
$F_l$	MW	Branch active power rating
$c_l^{fix}$	€/MW	Branch fixed cost
$\eta_{l,t}$		Efficiency loss of a branch
$x_l$		Reactance of line
$M_{l,c}$		Cycle matrix (here, $c$ represents cycle label)
$K_{i,l}$		Incidence matrix
$\pi_y$		Share of renewable generation
$C_y^{EC,lim}$	MW	Capacity limitation of energy carrier

Additional parameters and variables of the eFuels production		
Parameter/ variable	Unit	Description
$\alpha$		Scrubber unit labels
$\beta$		Direct air capture unit labels
$\gamma$		Electrolysis unit labels
$\delta$		Synthesis unit labels
$m_{l,t}^{FG,PS}$	t <sub>flue gas</sub>	Dispatch of flue gas point source
$C_{l,FG}$	t <sub>flue gas</sub> /h	Capacity of flue gas point source
$m_{l,t}^{CO_2,PS}$	t <sub>CO2</sub>	Dispatch of CO <sub>2</sub> point source
$C_{l,CO_2}$	t <sub>CO2</sub> /h	Capacity of CO <sub>2</sub> point source
$m_{\alpha,i,y,t}$	t <sub>flue gas</sub>	Dispatch of scrubber unit
$C_{\alpha,i,y}$	t <sub>flue gas</sub> /h	Capacity of scrubber unit
$c_{\alpha,i,y}^{fix}$	€/t <sub>flue gas</sub> * h	Fixed costs of scrubber unit
$c_{\alpha,i,y}^{var}$	€/t <sub>flue gas</sub>	Variable cost of scrubber unit
$\mu_{\alpha,i,y}$		Lower bound capacity utilization of scrubber unit
$\eta_{\alpha,i,y}^{FG,CO_2}$		Conversion efficiency scrubber
$m_{l,t}^{CO_2,SC}$	t <sub>CO2</sub>	CO <sub>2</sub> production from scrubber units
$p_{\beta,i,y,t}$	MW	Dispatch of DAC unit
$C_{\beta,i,y}$	MW	Capacity of DAC unit
$c_{\beta,i,y}^{fix}$	€/MW	Fixed costs of DAC unit
$c_{\beta,i,y}^{var}$	€/MWh	Variable cost of DAC unit
$\mu_{\beta,i,y}$		Lower bound capacity utilization of DAC unit
$\eta_{\beta,i,y}^{EL,CO_2}$		Conversion efficiency DAC
$m_{l,t}^{CO_2,DAC}$	t <sub>CO2</sub>	CO <sub>2</sub> production from DAC units
$m_{l,t}^{CO_2}$	t <sub>CO2</sub>	Total CO <sub>2</sub> production
$p_{\gamma,i,y,t}$	MW	Dispatch of electrolysis unit
$C_{\gamma,i,y}$	MW	Capacity of electrolysis unit
$c_{\gamma,i,y}^{fix}$	€/MW	Fixed costs of electrolysis unit
$c_{\gamma,i,y}^{var}$	€/MWh	Variable cost of electrolysis unit
$\mu_{\gamma,i,y}$		Lower bound capacity utilization of DAC unit
$\eta_{\gamma,i,y}^{EL,H_2}$		Conversion efficiency electrolysis
$p_{t,l}^{H_2}$	MWh	Total hydrogen production
$p_{\delta,i,y,t}^{H_2}$	MWh	Hydrogen dispatch of synthesis unit
$C_{\delta,i,y}$	MWh	Capacity of synthesis unit
$c_{\delta,i,y}^{fix}$	€/MW	Fixed costs of synthesis unit
$c_{\delta,i,y}^{var}$	€/MWh	Variable cost of synthesis unit

(continued on next page)

(continued)

Additional parameters and variables of the eFuels production		
Parameter/ variable	Unit	Description
$\mu_{\delta,i,y}$		Lower bound capacity utilization of synthesis unit
$\eta_{\delta,i,y}^{H_2,F}$		H <sub>2</sub> Conversion efficiency FTS
$m_{\delta,i,y,t}^{CO_2}$	tCO <sub>2</sub>	CO <sub>2</sub> dispatch of synthesis unit
$\eta_{\delta,i,y}^{CO_2,F}$		CO <sub>2</sub> Conversion efficiency FTS
$p_{\delta,i,y,t}^F$	MWh	Fuel dispatch of synthesis unit
$p_{i,t}^F$	MWh	Total fuel production
$D_y^{F,tot}$	MWh	Total fuel demand
Sets		
GEN		Generators
EC		Energy carrier
HC		Hard coal power plants
RES		Renewable energy sources
HS		Hydrogen storage

#### 4.1. Description of the energy system model

In this paper, we use the open-source energy system toolbox PyPSA (Brown et al., 2018) and the PyPSA-EUR workflow (Hörsch et al., 2018a) to implement the fundamental energy system model which we then extend to account for eFuels. PyPSA allows several applications, including ones considering electricity network restrictions based on a DC formulation using a linearized optimal power flow.

While the framework used only allows for the optimization of a static timeframe with multiple time steps, the investigation of the effect of electricity purchase conditions on the energy system requires the consideration of multiple linked years. Thus, the existing formulation is extended by a subsequent multi-year implementation to analyze the development of the energy system over the considered time frame using multiple optimization years. The implementation of the time coupling process is shown in Fig. 1. The model extension allows the detailed investigation of expansion planning of the grid, electricity generation, and eFuels production over a multi-year time horizon under the consideration of the interconnection between installation times of renewable energies and electrolysis units.

##### 4.1.1. Objective function

In PyPSA, the total annual system costs are minimized. The system cost contains variable and fixed costs of generation, storage and transmission. In addition, we consider the capital and operating costs of eFuel production. Unit commitment is not considered. The objective function is given by Equation (1).

$$\begin{aligned} \min \sum_t c_t^{fix} \cdot F_t + \sum_i \sum_y \left( \sum_u \left( c_{u,i,y} \cdot c_{u,i,y}^{fix} + \sum_t \omega_t \cdot g_{u,i,y} \right. \right. \\ \left. \left. \cdot c_{u,i,y}^{var} \right) + \sum_\alpha \left( c_{\alpha,i,y} \cdot c_{\alpha,i,y}^{fix} + \sum_t \omega_t \cdot m_{\alpha,i,y,t} \cdot c_{\alpha,i,y}^{var} \right) + \sum_\beta \left( C_{\beta,i,y} \right. \right. \\ \left. \left. \cdot c_{\beta,i,y}^{fix} + \sum_t \omega_t \cdot p_{\beta,i,y,t} \cdot c_{\beta,i,y}^{var} \right) + \sum_\gamma \left( C_{\gamma,i,y} \cdot c_{\gamma,i,y}^{fix} + \sum_t \omega_t \cdot p_{\gamma,i,y,t} \right. \right. \\ \left. \left. \cdot c_{\gamma,i,y}^{var} \right) + \sum_\delta \left( C_{\delta,i,y} \cdot c_{\delta,i,y}^{fix} + \sum_t \omega_t \cdot p_{\delta,i,y,t}^{H_2} \cdot c_{\delta,i,y}^{var} \right) \right) \end{aligned} \quad (1)$$

##### 4.1.2. Constraints

To model the technical constraints of the basic electrical components of the energy system, Equations (2)–(8) are used. In the case of generators and storages, Eq. (2) describes the lower and upper limit of the generator dispatch. In the case of RES generators,  $\bar{g}_{u,i,y,t}$  describes the availability of the renewable energy at the location at each time step. The capacities of the generators are limited by lower and upper capacity

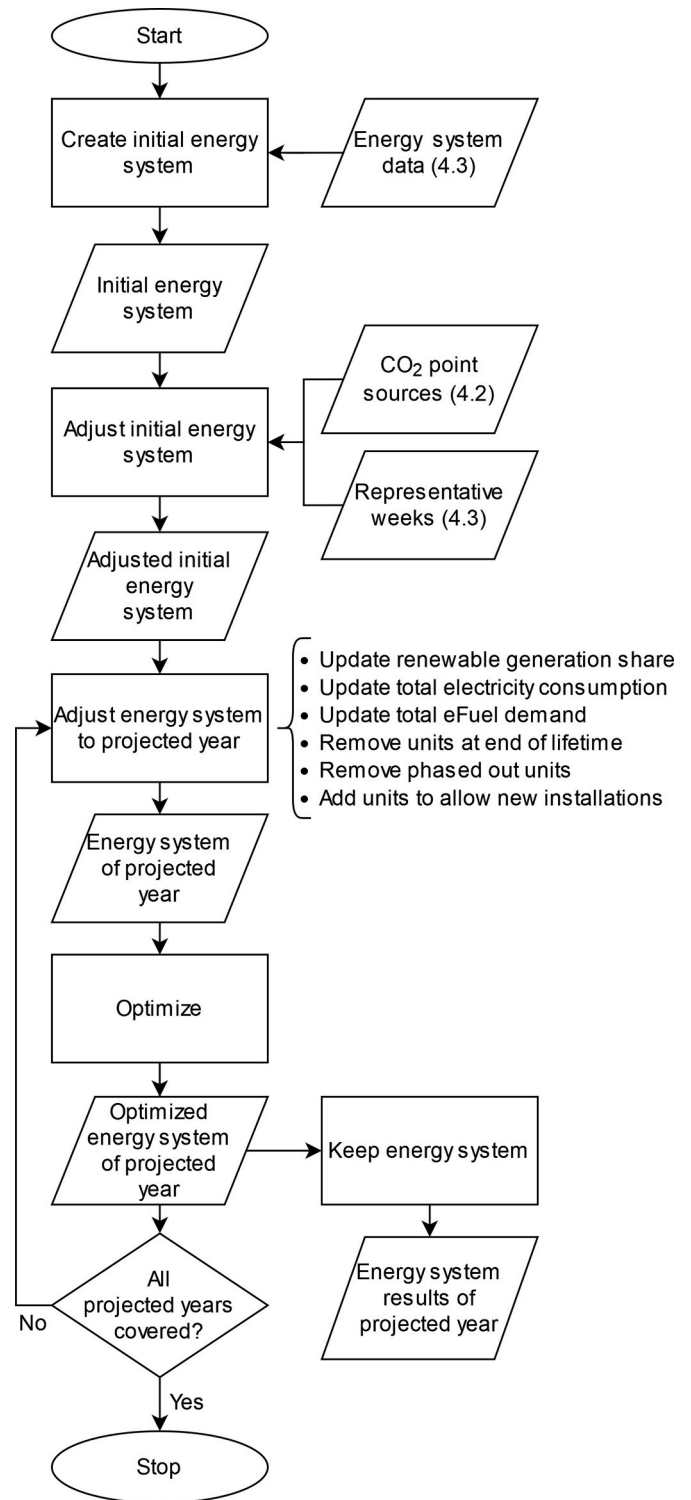


Fig. 1. Flow chart of the time coupling process.

limits (3). This equation accounts for renewable generators limited by renewable potential at the location. Eq. (4) defines the ramp-up and ramp-down limitations of the generator dispatch.

$$\tilde{g}_{u,i,y,t} \cdot C_{u,i,y} \leq g_{u,i,y,t} \leq \bar{g}_{u,i,y,t} \cdot C_{u,i,y} \forall u, i, y, t \quad (2)$$

$$\tilde{C}_{u,i,y} \leq \sum_y C_{u,i,y} \leq \bar{C}_{u,i,y} \forall u, i \quad (3)$$

$$-rd_{u,i,y} \bullet C_{u,i,y} \leq (g_{u,i,y,t} - g_{u,i,y,t-1}) \leq ru_{u,i,y} \bullet C_{u,i,y} \forall u, i, y, t > 1 \quad (4)$$

For each time step, the energy level of the previous time step, the charging and discharging, as well as inflows and spillage are taken to calculate the energy level of a storage unit at the current time step (5). Eq. (6) defines the range of the energy level of each storage.

$$e_{u,i,y,t} = \eta_{u,i,y,0}^{\text{in}} \bullet e_{u,i,y,t-1} + \eta_{u,i,y,+} \bullet \omega_t [g_{u,i,y,t}]^+ - \eta_{u,i,y,-}^{-1} \bullet \omega_t [g_{u,i,y,t}]^- + \omega_t \bullet g_{u,i,y,t}^{\text{in}} - \omega_t \bullet g_{u,i,y,t}^{\text{spill}} \forall u, i, y, t \quad (5)$$

$$\tilde{e}_{u,i,y,t} \bullet E_{u,i,y} \leq e_{u,i,y,t} \leq \bar{e}_{u,i,y,t} \bullet E_{u,i,y} \forall u, i, y, t \quad (6)$$

Kirchhoff's current law is implemented in the energy system balance using Eq. (7). It ensures that the inelastic demand is covered by the total generator dispatch, the storage dispatch, and the flows through branches, differentiated in controllable links and passive lines from other buses at every bus and at each time step (Frysztacki et al., 2021).

$$\sum_u g_{u,i,y,t} + \sum_l K_{il} f_{l,t} = d_{i,t} \forall i, l, y, t \quad (7)$$

The link and line dispatch are limited by time-dependent availability ( $\tilde{f}_{l,t} = -1$  and  $\bar{f}_{l,t} = 1$  in the case of lines) and the respective capacity (8).

$$\tilde{f}_{l,t} \bullet F_l \leq f_{l,t} \leq \bar{f}_{l,t} \bullet F_l \forall l, t \quad (8)$$

Finally, Kirchhoff's voltage law is implemented with Eq. (9). The linear load flow implementation allows for a good approximation of the transmission network and the implementation, as cycle constraints have a lower computational effort compared to angle- or PTFD-based formulations (Hörsch et al., 2018b; Frysztacki et al., 2021).

$$\sum_l M_{l,c} \bullet x_l \bullet f_{l,t} = 0 \forall c, t \quad (9)$$

To extend on the fundamental model described in this section, additional constraints to specify the energy system's transition path are implemented. Eq. (10) limits the total capacity of generators that use a specific energy carrier. This equation allows for the implementation of a national policy aimed at reducing electricity generation from certain energy carriers. Eq. (11) further restricts the transition pathway towards renewable energy sources by defining a lower bound for renewable electricity generation share of  $\pi_y$ . Both parameters, the capacity limit of generators ( $C_y^{\text{EC,lim}}$ ) and the renewable electricity generation share ( $\pi_y$ ) depend on the currently processed projected year.

$$C_y^{\text{EC,lim}} \geq \sum_u \sum_i \sum_y \bar{C}_{u,i,y} \forall y \quad (10)$$

$$\pi_y \sum_u \sum_i \sum_y \sum_t (g_{u,i,y,t} \bullet \omega_t) \leq \sum_u \sum_i \sum_y \sum_t (g_{u,i,y,t} \bullet \omega_t) \quad (11)$$

## 4.2. eFuel production

The following chapter introduces the considered PtL route and describes its implementation in the overall modelling framework. One mandatory element of the eFuels production is the provision of CO<sub>2</sub>. We assume that CO<sub>2</sub> can be obtained from point sources and DAC. Point sources have the advantage that the emitted flue gas consists of a high concentration of CO<sub>2</sub> or pure CO<sub>2</sub>. Their limitation is the capacity of the point source. DAC, on the other side, allows CO<sub>2</sub> supply from ambient air, which provides the possibility to gather much larger quantities of CO<sub>2</sub>. However, the lower CO<sub>2</sub> concentration in the air results in higher energy demands for the separation process. Scrubber units and DAC are assumed low-temperature units, allowing for heat utilization of the

synthesis processes without further heat supply. The second input for eFuels production is hydrogen. Here, we model the electrolysis as a polymer electrolyte membrane (PEM), as this technology is able to react immediately to volatile electricity generation and the output hydrogen has a favorable pressure level for the following synthesis steps. The actual synthesis is implemented as a single component. This component includes the supply of synthesis gas via reverse water-gas shift reaction, the FTS step to produce the syncrude, and the product processing in the hydrocracker. The process is connected to the electricity grid and a battery storage unit can be used for more flexibility either in the energy system or the PtL process. Fig. 2 depicts the implemented PtL process.

Similar to generators, the output of the CO<sub>2</sub> point source  $m$  is limited by the capacity of the point source. Ramp-up and ramp-down constraints, or dispatch limitations, are not applied, as it is assumed that excess flue gas or CO<sub>2</sub> can be emitted if necessary. Eqs. (12) and (13) describe the limiting constraints.

$$0 \leq m_{i,t}^{\text{FG,PS}} \leq C_{i,\text{flue gas}} \forall i, t \quad (12)$$

$$0 \leq m_{i,t}^{\text{CO}_2,\text{PS}} \leq C_{i,\text{CO}_2} \forall i, t \quad (13)$$

The DAC utilization is limited by the capacity of the DAC (14). Heat demand is not considered as it can be covered by the exothermal reactions of the synthesis units. Furthermore, ambient air is sufficiently available and, therefore, excluded in the optimization program. The electricity consumption of the DAC unit is taken into account with Eq. (15). This demand originates mainly from the operation of the ventilators that direct the ambient air through the separation unit.

$$0 \leq p_{\beta,i,y,t} \leq C_{\beta,i,y} \forall \beta, i, y, t \quad (14)$$

$$m_{i,t}^{\text{CO}_2 \text{ from DAC}} = \sum_{\beta} \sum_y (p_{\beta,i,y,t} \bullet \eta_{\beta,i,y}^{\text{EL,CO}_2}) \forall i, t \quad (15)$$

Similar to the utilization limitation in the case of DAC units, CO<sub>2</sub> scrubber units are limited as well (16). The total production of CO<sub>2</sub> from the scrubber units at each bus depends on the used flue gas and the conversion factor (17). Heat demand, again, is not considered. Eq. (18) limits the flue gas used by the scrubber units to the total available flue gas of all point sources at each hour and each bus. The total volume of CO<sub>2</sub> available at each hour and each bus is modelled in Eq. (19). The equation describes the contribution of CO<sub>2</sub> from DAC, point sources with scrubber unit, and point sources with direct CO<sub>2</sub> emissions to the total CO<sub>2</sub> available.

$$0 \leq m_{\alpha,i,y,t}^{\text{FG,PS}} \leq C_{\alpha,i,y} \forall \alpha, i, y, t \quad (16)$$

$$m_{i,t}^{\text{CO}_2,\text{SC}} = \sum_{\alpha} \sum_y (m_{\alpha,i,y,t}^{\text{FG,PS}} \bullet \eta_{\alpha,i,y}^{\text{FG,CO}_2}) \forall i, t \quad (17)$$

$$m_{i,t}^{\text{FG,PS}} = \sum_{\alpha} \sum_y m_{\alpha,i,y,t}^{\text{FG,PS}} \forall i, t \quad (18)$$

$$m_{i,t}^{\text{CO}_2} = m_{i,t}^{\text{CO}_2,\text{PS}} + m_{i,t}^{\text{CO}_2,\text{SC}} + m_{i,t}^{\text{CO}_2,\text{DAC}} \forall i, t \quad (19)$$

The operation of the electrolysis is described with Eq. (20) and Eq. (21). Eq. (20) describes the dispatch limitation of the electrolysis. Due to the high flexibility of electrolysis, the operation of the unit is only constrained by its capacity. Eq. (21) treats the conversion of electricity to hydrogen by implementing the efficiency of the electrolysis. The conversion of distilled water to hydrogen is not covered. Instead, the costs of distilled water is included in the operational costs of the electrolysis.

$$0 \leq p_{\gamma,i,y,t} \leq C_{\gamma,i,y} \forall \gamma, t, y, t \quad (20)$$

$$p_{i,t}^{\text{H}_2} = \sum_{\gamma} \sum_y (p_{\gamma,i,y,t} \bullet \eta_{\gamma,i,y}^{\text{EL,H}_2}) \forall i, t \quad (21)$$

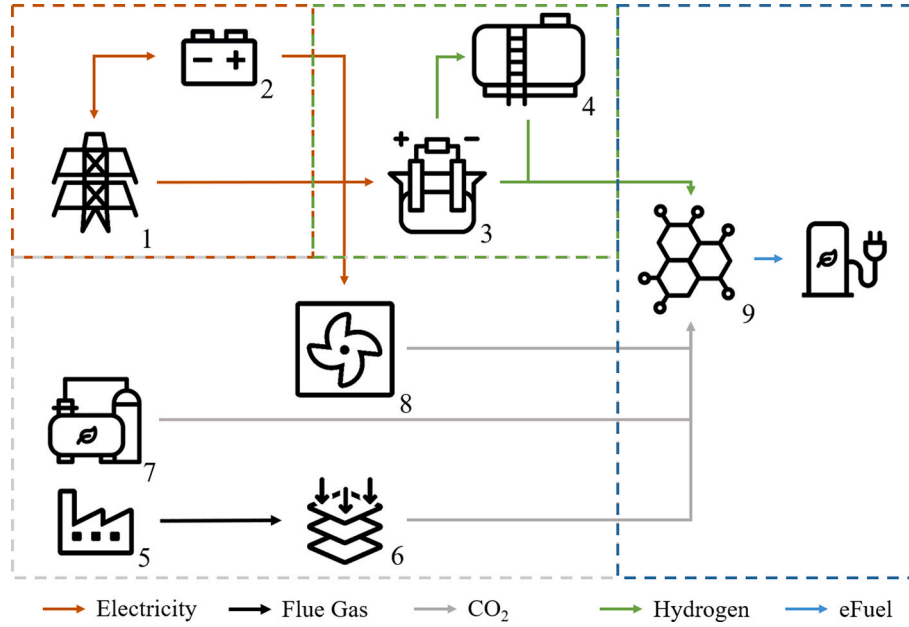


**Fig. 2.** Schematic structure of the power-to-liquid Fischer-Tropsch route comprising the energy system (1), battery storage (2), PEM electrolysis (3), hydrogen storage (4), flue gas point sources (5), scrubber unit (6), direct CO<sub>2</sub> point sources (7), direct air capture unit (8) and synthesis unit (9). The different arrow colors represent the different energy and mass flows: orange represents electricity, green represents hydrogen, black represents flue gas, grey represents CO<sub>2</sub> and blue represents eFuel.

Eq. (22) implements the dispatch limitation of the synthesis unit. The conversion of hydrogen to fuel is covered in Eq. (23). To connect the synthesis unit to the hydrogen storage and electrolysis, Eq. (24) balances the hydrogen at the bus using hydrogen production and consumption, and storage dispatch. Similar to the hydrogen, CO<sub>2</sub> conversion is covered in Eq. (25). As no CO<sub>2</sub> storage exists, only CO<sub>2</sub> production and consumptions needs to be balanced at each time step. This is implemented with Eq. (26). Finally, the total fuel production at the bus and time step is calculated using Eq. (27).

$$\mu_{\delta,i,y} \cdot C_{\delta,i,y} \leq p_{\delta,i,y,t}^{H_2} \leq C_{\delta,i,y} \forall \delta, i, y, t \quad (22)$$

$$p_{\delta,i,y,t}^F = p_{\delta,i,y,t}^{H_2} \cdot \eta_{\delta,i,y}^{H_2,F} \forall \delta, i, y, t \quad (23)$$

$$p_{i,t}^{H_2} + \sum_u \sum_y g_{u,i,y,t} = \sum_\delta \sum_y p_{\delta,i,y,t}^{H_2} \forall i, t \quad (24)$$

$$p_{\delta,i,y,t}^F = m_{\delta,i,y,t}^{CO_2} \cdot \eta_{\delta,i,y}^{CO_2,F} \forall \delta, i, y, t \quad (25)$$

$$m_{i,t}^{CO_2} = \sum_\delta \sum_y m_{\delta,i,y,t}^{CO_2} \forall i, t \quad (26)$$

$$p_{i,t}^F = \sum_\delta \sum_y p_{\delta,i,y,t}^F \forall i, t \quad (27)$$

The total yearly eFuels production of the FTS units has to be equal or larger than the total yearly demand. This constraint is implemented with Eq. (28). As hydrogen cannot be obtained from sources other than electrolysis, and CO<sub>2</sub> cannot be obtained from sources other than DAC, flue gas scrubber units or direct CO<sub>2</sub> sources, this constraint will force the optimization to calculate the optimal capacities of storages, electrolysis, CO<sub>2</sub> supply, and synthesis units. Additionally, the dispatch is optimized to cover the eFuels demand set in this constraint.

$$D_y^{F,tot} \leq \sum_i \sum_t p_{i,t}^F \cdot \omega_t \forall y \quad (28)$$

### 4.3. Electricity purchase condition constraints and implementation methods

The primary intention of this approach is to analyze the impact of electricity purchase conditions in eFuel production and the energy system. Thus, in the following subchapter we explain the implementation of the purchase conditions of origin, additionality and correlation into the presented approach.

#### 4.3.1. Renewable origin

If the PtL facility is grid-connected, Art.4(2) defines that power purchase agreements have to be contracted to ensure the renewable origin of the eFuel. In the model formulation described above, all PtL facilities are grid-connected. Therefore, it is assumed that power purchase agreements are used for all PtL facilities.

#### 4.3.2. Element of additionality

Eq. (11) defines that at least the share  $\pi_y$  of the total electricity generation is covered by renewable generation. Following only this system boundary, it would not be necessary to cover electricity demand of electrolysis units with renewable energy entirely, which does not fulfill the renewable origin criteria as a purchase criteria. Therefore, electricity consumption of electrolysis units is added to the total renewable share objective with share  $(1 - \pi_y)$ . This increased share satisfies two requirements simultaneously because the element of additionality as the increased electricity demand, caused solely by the electrolysis units, will be covered entirely by RES. If the electricity purchase conditions are considered, Eq. (29) replaces Eq. (11) which leads to the previously described result of fulfilling the element of additionality.

$$\begin{aligned} & \pi_y \sum_u \sum_i \sum_y \sum_t (g_{u,i,y,t} \cdot \omega_t) + (1 - \pi_y) \sum_\gamma \sum_i \sum_y \sum_t (p_{\gamma,i,y,t} \cdot \omega_t) \\ & \leq \sum_u \sum_i \sum_y \sum_t (g_{u,i,y,t} \cdot \omega_t) \end{aligned} \quad (29)$$

#### 4.3.3. Temporal and geographical correlation

The placement of RES generation and PtL facility in the same bidding zone is one way of defining the geographical correlation in the European electricity market. This market is characterized by multiple bidding zones which borders should largely align with congested lines of the transmission system. In this context, congestions between the supply and demand of electricity should be avoided by restricting the investment of RES generation and PtL to the same bidding zone. Currently, unified pricing areas like Germany are subject to internal congestions and are resolving these with measures of congestion management after the market has been cleared. Therefore, the approach using only bidding zones does not fully satisfy the requirements in situations where significant congestion occurs within a bidding zone. While the current legislative proposal on a European basis does not go beyond the definition of geographical correlation on bidding zone level, it seems reasonable to assume that additional constraints which further restrict placement of RES generation and PtL location will be implemented in countries with internal grid congestion like Germany. Thus, we model the geographical correlation in a more restricting way based on a nodal correlation approach. This can be achieved by limiting electrolysis electricity consumption in a network node to the available RES generation at the same network node. While this approach can be considered as a significant exceedance of the zonal restriction, it provides a much more efficient boundary to achieve the goal of the geographical correlation as a purchase condition in Europe during the transition phase towards a carbon neutral energy system.

Electrolysis units present the issue that uncontrolled electricity consumption could stress the electricity grid additionally. In addition, unconstrained electricity consumption might result in high carbon footprints of the produced hydrogen if the production takes place during hours with a high share of electricity generation from carbon-based energy carriers. The temporal correlation requirement aims to avoid both challenges. It constrains the electricity consumption of electrolysis to the electricity generation from the associated RES on an hourly basis.

Eq. (30) shows the combined temporal and geographical correlation constraint. For each network node and hour step, electricity consumption of electrolysis units at the same bus has to be smaller than or equal to electricity generation from RES at this bus. In addition, electricity consumption of electrolysis units is constrained to RES capacities that have been installed in the same projected year (considering  $y$ ), adhering the electricity purchase to the additionality constraint.

$$\sum_y p_{r,i,y,t} \leq \sum_u^{RES} g_{u,i,y,t} \forall i, t, y \quad (30)$$

## 5. Case study

### 5.1. Scenarios

The case study consists of three scenarios, which all are investigated using the optimization approach described in Chapter 3. The three scenarios differ regarding eFuel production objective and the set of applied electricity purchase conditions. The first scenario depicts the reference case and uses neither eFuel production objectives nor electricity purchase conditions. The results can be considered as the benchmark energy system which results from no future requirement for eFuel production and subsequently no conditions for such production. The benchmark results will be used to discuss changes following the eFuel production implementation in the two other scenarios. In the second scenario, *No-RED*, the eFuel production objective is implemented as a constraint (Eq. (28)) to assure production of the desired amount of eFuels while electricity purchase conditions are not applied. Lastly, in the third scenario, *RED*, the eFuel production objective and electricity purchase conditions constraints proposed in the legislation of RED II are both added with the subsequent restrictions to the performed

optimization. Here, the electricity purchase conditions apply for the projected years 2025 and 2030 to account for the transitional phase. Additionally, we implement this scenario with the hourly temporal correlation starting already before 2030 which is optional for all member states.

Eq. (30) constrains the eFuels production to RES. We further constrain Eq. (30) to wind and solar generation only, instead of all RES. Electricity from hydropower is excluded as the hydropower potential in Germany is already utilized and no further hydropower plants can be build. Biomass is excluded because the direct utilization of biomass to produce biofuels is more efficient than the route via electricity generation to produce eFuels.

All scenarios consider the phase-out of nuclear and coal power plants. Nuclear and lignite power plants are decommissioned with individual deconstruction dates based on the national phase-out schedule. The total hard coal power plant capacity is limited through Eq. (10), resulting in an optimized hard coal decommissioning schedule from an overall system perspective (see Chapter 4.3).

### 5.2. CO<sub>2</sub> sources

The availability of CO<sub>2</sub> sources is a fundamental element for determining the optimal location of eFuel production. While there are a large variety of potential CO<sub>2</sub> sources that can be utilized in the process of producing eFuels, a small number of industries and industry sectors provide the majority of this potential and are of most interest when creating a dataset of CO<sub>2</sub> sources. Consequently, we use a geographically matched dataset of steel factories, refineries, cement factories, bioethanol plants, and biomethane plants as available CO<sub>2</sub> or flue gas sources. These sources are process-related and thus especially favorable for utilization in the eFuels production process as they cannot be avoided by using renewable energy carriers. Energy-related CO<sub>2</sub> emissions derive from the combustion of lignite, coal, natural gas or crude oil to supply energy as heat or electricity. Using energy-related CO<sub>2</sub> emissions has several shortcomings. For one, CO<sub>2</sub> emissions would not be carbon neutral. Additionally, the added steps of combustion and electricity generation would reduce the overall efficiency of the PtL process further. These energy carriers could be converted directly into fuels using gasification or pyrolysis, achieving a higher efficiency. Therefore, energy-related CO<sub>2</sub> emissions are not considered.

To derive the final CO<sub>2</sub> emissions, we preprocess the data of the different technologies. In the case of steel factories, refineries, and cement factories, the total yearly emissions of each facility are reduced by energy-related emissions. For bioethanol plants, no information on their emissions is available. Therefore, we use the capacities of the bioethanol plants in combination with a specific CO<sub>2</sub> emission of 0.96 tons of CO<sub>2</sub> per produced ton of bioethanol (Meisel et al., 2015) to calculate the total yearly CO<sub>2</sub> emissions of each bioethanol plant. The problem of missing data availability on CO<sub>2</sub> emissions also exists for biomethane plants. Typically, CO<sub>2</sub> concentration of biomethane plants lie between 25% and 45% (Fischedick et al., 2015). Based on this range, we use an average CO<sub>2</sub> concentration of 35% and the facility capacity to calculate the yearly CO<sub>2</sub> emissions. The total yearly CO<sub>2</sub> emissions are assumed to be equally distributed over the year, allowing for the calculation of hourly CO<sub>2</sub> emissions. Table 1 shows yearly and hourly CO<sub>2</sub> emissions of the considered emitters, and Fig. 3 shows the spatial distribution of the facilities within Germany.

### 5.3. Energy system input data

Data on the German transmission grid, conventional generators, distribution of electricity demand, as well as renewable generation profiles are based on the PyPSA-EUR energy system workflow (Hörsch et al., 2018a). We extended data of RES capacities based on the core energy market data (Bundesnetzagentur, 2021) of the German federal network agency and matched this data with the data provided by

**Table 1**  
Yearly and hourly flue gas and CO<sub>2</sub> point source emissions.

Facility	Hourly Emissions [t/h]	Yearly Emissions [Mio. t]	Emission type	Reference
Steel factory	5165	45.24	Flue gas	<a href="http://www.thru.de">www.thru.de</a> (Deutsche Emissionshandelsstelle, 2021)
Refinery	2512	22.00	Flue gas	<a href="http://www.thru.de">www.thru.de</a> (Deutsche Emissionshandelsstelle, 2021)
Cement factory	2495	21.85	Flue gas	<a href="http://www.thru.de">www.thru.de</a> (Deutsche Emissionshandelsstelle, 2021)
Bioethanol plant	176	1.54	CO <sub>2</sub>	Bundesverband der deutschen Bioethanolwirtschaft e. V. (2021)
Biomethane plant	142	1.24	Flue gas	Deutsche Energie-Agentur (2021)

PyPSA-EUR. To reduce the computational intensity and account for the yearly, weather-dependent variation in electricity demand and volatile RES generation, the profiles of demand and renewable capacity factors are included using representative weeks. Here, historical data from 2012 to 2019 is clustered to derive nine representative weeks for each calculated year using the clustering approach proposed in Yilmaz et al. (2019). The resulting representative week consists of load and renewable capacity factor profiles, which are individually weighted using the time step weighting  $\omega_t$  to create a representative sample of the demand and generation patterns of the last seven years. Figure 4 shows the

different data sets and their underlying structure for the year 2020.

To achieve the development of a high RES energy system, following time-dependent parameters are used: First, the renewable generation share of the total electricity generation. This parameter aims to steadily increase the RES capacities and generation. The net power consumption defines the total electricity consumption within the energy system. This consumption increases due to increasing consumers like heat pumps, electric vehicles, and other power-to-x applications like hydrogen and methane production (power-to-gas). The generating hard coal capacities are limited by the hard coal capacity limitation set by the German government. All described assumptions are given in Table 2.

#### 5.4. eFuel production in Germany

The eFuel production in Europe heavily relies on the development of the energy system, political support and the development of eFuel production technologies. From the energy system point of view, hydrogen and eFuel production are especially useful if the renewable potential allows low-cost production. In countries like Germany, renewable potentials are limited and the eFuel production is in direct competition to the coverage of conventional load, electric mobility and other electricity-based applications. Looking at the political aspects, a general hesitation towards eFuels is noticeable. For example, the planned crediting system in RED II enables national members to develop a technology-based strategy to reduce GHG emissions. This crediting system might favor technologies like electric mobility or (advanced) biofuels as they can be credited multiple times, giving them a larger lever to reduce GHG emissions than eFuels. In addition, car manufacturers need to reduce the tail pipe emissions of their fleet to 0 g CO<sub>2</sub> equivalents per kilometer by 2035. eFuels are only a valid option if the

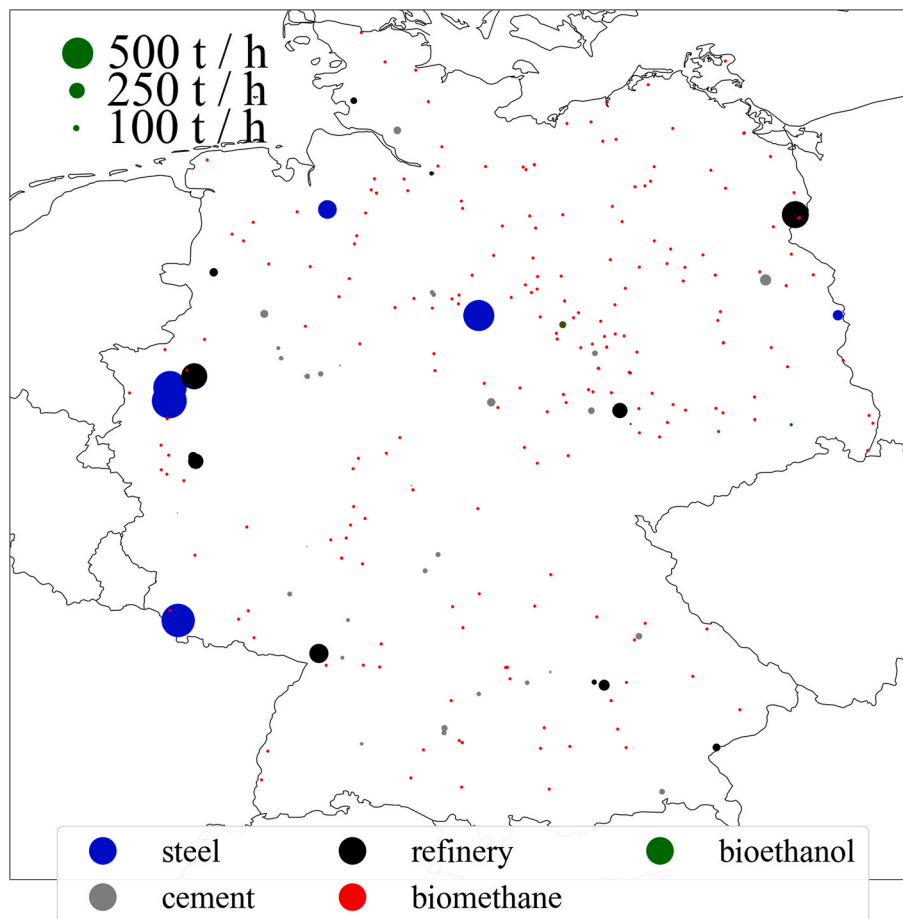


Fig. 3. Distribution of flue gas and CO<sub>2</sub> point source capacities in Germany.

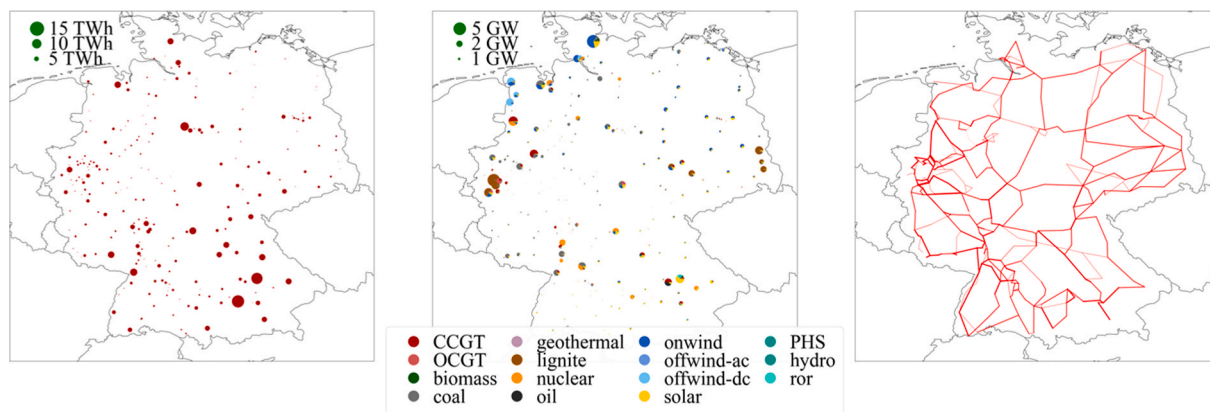


Fig. 4. Distribution of yearly spatial load demand (left), generator capacity (middle) and transmission lines (right) in 2020.

Table 2

Assumptions on renewable generation share, total power consumption and hard coal generator capacity limits.

Parameter	2020	2025	2030	Reference
Renewable generation share	40%	54%	68%	Sensfuß et al. (2021)
Net power consumption [TWh]	532,8	589,9 (interpolated)	647	Sensfuß et al. (2021)
Hard coal capacity limit	–	9.9 GW	8 GW	Bundesamt für Justiz (8/14/2020)

internal combustion engine vehicle exclusively uses eFuels, banning drop-in fuels with only a share of eFuels completely. Next to the policy aspects, technological uncertainties exist. Electrolysis and DAC are still immature technologies, which gives rise to the question if large capacities of these technologies will be available to supply large volumes of eFuels. In addition, due to the necessity of electrolysis in the eFuels production process, the production of eFuels is in direct competition to other technologies that depend on electrolysis and green hydrogen. This includes, for example, steel production, refinery processes, the pharmaceutical, chemical and agricultural industry. This situation might further reduce the support by policy makers as this competition could slow down GHG emission reduction efforts in these sectors. Furthermore, looking at the current projects in the fields of eFuels, the majority of large-scale projects are planned at locations with favorable renewable energy generation outside of Germany or even outside of Europe to achieve low production costs. Therefore, it is assumable that the majority of eFuels will be produced outside of Germany and will not be covered by domestic production. Based on the above-mentioned aspects and uncertainties, we conclude that only little domestic eFuels volume will take place in Germany and assume that larger volumes will be produced outside of Germany.

The policy framework ReFuels Aviation (European Union 4/25/2023) implements a eFuels quota of 1.2% in 2030 and 2% in 2032 in the aviation sector. It is important to mention that even this quota does not mean that the eFuels are produced in Germany. Distribution companies like refineries are obligated to distribute the quota of aviation fuels as eFuels, but are not bounded to produce these in Germany. To analyze the impact of the eFuel scale-up, we assume an eFuel production of 0.5% in 2025–2029, and 2% starting in 2030. Based on the aviation fuel demand in Germany in 2019 (434 PJ (Arbeitsgemeinschaft Energiebilanzen e.V., 2021)), and assuming that this demand remains constant, around 0.6 and 2.41 TWh of eFuel will be needed by 2025 and 2030, respectively, to meet the quota. Consequently, these values are used as the eFuel production objective for this case study.

## 6. Results & discussion

### 6.1. eFuel production facilities

#### 6.1.1. Electrolysis, synthesis and storage capacity

Table 3 provides an overview of the total electrolysis, synthesis and storage capacities. Without any restrictions from electricity purchase conditions (No-RED), total electrolysis capacities will reach 201 MW by 2025 and 1128 MW by 2030. The increasing eFuel demand drives the growing electrolysis capacity in this scenario. In the RED scenario, this additional electricity demand has the same effect but the additional purchase conditions lead to increased total electrolysis capacities of 220 MW in 2025 and 1306 MW in 2030. Altogether, the RED II conditions result in 9.0% more electrolysis capacity in 2025 and 15.8% more electrolysis capacity in 2030.

At the same time, the total capacity of synthesis units will reach very similar levels in both scenarios. The main reason is that the synthesis is not highly flexible, and the operation is not constrained in both scenarios. However, while synthesis capacities develop almost consistently, storage capacities differ strongly. Due to low flexibility and the inability to shut down synthesis units, situations with a low electricity supply, that would result in reduced or stopped hydrogen production, need to be bridged by hydrogen supply from hydrogen storage. The resulting hydrogen storage in the No-RED scenario is capable of supplying hydrogen for the synthesis process for 30.06 h in 2025 and 55.50 h in 2030. In the RED scenario, these numbers increase to 54.8 h in 2025 and 111.2 h in 2030.

#### 6.1.2. Operation of electrolysis units

In the No-RED scenario, electrolysis units have an average utilization of 7984 h in 2025 and 5875 h in 2030. Even though electrolysis operation is not constrained, electrolysis units are not operated at full utilization in 2025 and 2030. With decreasing fixed costs of electrolysis and an increasing share of renewable energy over the years, offering flexibility from electrolysis overcapacities becomes more attractive as average local marginal prices decrease with a higher share of RES. This decreased utilization further explains the increase of the storage capacity to synthesis capacity ratio. With lower utilization and a steady demand for synthesis, more hydrogen needs to be stored to bridge gaps

Table 3

Capacities of electrolysis, synthesis units and hydrogen storage in the No-RED and RED scenarios.

Parameter	No-RED		RED	
	2025	2030	2025	2030
Total Electrolysis Capacity [MW Electricity]	201	1128	220	1306
Total Synthesis Capacity [MW Hydrogen]	69	298	69	285
Total Hydrogen Storage Capacity [MWh]	2071	16,532	5860	31,646

without hydrogen production.

Purchase condition constraints result in lower utilization of electrolysis units in the RED scenario. The associated dispatch results in lower utilization of 7336 h in 2025 and 5203 h in 2030. Similarly to the No-RED scenario, this effect can be attributed to lower marginal prices and decreasing cost of electrolysis units. However, the even-higher reduction in electrolysis utilization is caused by the time-dependent availability of RES generation. Altogether, the utilization drops by 8.1% in 2025 and 11.4% in 2030.

The operation of electrolysis is illustrated in Fig. 5 (No-RED) and Fig. 6 (RED). To compare the dispatch, one network node is chosen, where the installation of electrolysis capacity is optimal in the No-RED and RED scenarios. Both figures use a logarithmic scale on the y-axis to allow for comparison of the dispatch as the renewable capacities differ.

Fig. 5 shows the dispatch of the electrolysis unit and the available RES generation at the chosen network node in the No-RED scenario without electrolysis dispatch constraints. The electrolysis unit is dispatched at maximum capacity at the majority of time steps and is not affected by the RES generation directly. Indirectly, electrolysis utilization is influenced by low marginal prices of electricity, which occur when renewable energy generation is high and conventional electricity demand is low. In addition, biomass-based electricity generation is available to operate the eFuel production facility.

Fig. 6 shows the exemplary electrolysis unit in the RED scenario and the corresponding RES generation. Corresponding RES capacities are only such, which have been commissioned in the same projected year as the electrolysis and, therefore, meet the additionality requirement. Two things are observable. On the one hand, the corresponding RES generation is much smaller than the total available RES capacities at the network node as seen in Fig. 5. This limitation derives from the additionality constraint. On the other hand, it is apparent that the operation is increasingly correlated to the corresponding RES generation, which results in shutdowns of the electrolysis unit when wind and solar generation are insufficient to satisfy the nodal electrolysis demand. This correlation derives from the temporal correlation. Even though generation of wind and solar capacities commissioned in the same projected year is sufficient during many hours to operate the electrolysis at high utilization levels, the electrolysis stops operation for short periods before and after solar generation. The volatile operation is caused by low marginal prices, which shapes the electrolysis operation curve. This can be seen by the reduction of electrolysis operation in a corresponding manner to the reduction of solar generation. Another interesting point is the high utilization of the electrolysis shown in Fig. 6 and numerically presented in Table 4. This high utilization is possible due to the ratio between electrolysis and RES capacities. The system feeds in the residual energy between RES generation and electrolysis demand into the

electricity grid. This approach allows high electrolysis utilization even with limited RES potential and might be a suitable approach for eFuels production under the RED II regime.

### 6.1.3. CO<sub>2</sub> source

The results show that the application of the energy purchase conditions result in different utilization of the CO<sub>2</sub> production technologies. In the No-RED scenario in 2025, almost all CO<sub>2</sub> is obtained from direct sources, and even in 2030, direct sources supply 46.91% of the total CO<sub>2</sub>. DAC plays no role in the No-RED scenario. In the RED scenario, the CO<sub>2</sub> supply is more diversified. In 2025, the major share is CO<sub>2</sub> from sources with flue gas (68.2%), followed by direct sources (30.6%), and DAC (1.2%). In 2030, CO<sub>2</sub> from direct sources does not increase, while DAC CO<sub>2</sub> increases by 14.307 tons. Nevertheless, the major share of CO<sub>2</sub> is still scrubbed from flue gas sources, accounting for 89.9% of the total CO<sub>2</sub>.

The distribution of CO<sub>2</sub> production technologies in Fig. 7 shows that CO<sub>2</sub> sources play an important role next to the electricity supply. Without the constrained electricity supply, direct sources play a significant role and locations are chosen based on the available CO<sub>2</sub>. With the implementation of RED II constraints, electricity purchase is more constrained, and fewer locations are attractive regarding electricity supply. Instead of implementing production facilities at direct CO<sub>2</sub> sources like in the No-RED scenario, the energy system in the RED scenario prioritizes the electricity supply over the CO<sub>2</sub> supply and accepts a less attractive CO<sub>2</sub> supply. Simultaneously, this shift towards prioritized electricity supply leads to the increased relevance of DAC, as CO<sub>2</sub> sources are often limited at the locations with the most attractive, RED II adhered electricity supply, which does not influence DAC at the same time.

### 6.1.4. Production facility locations

The above-mentioned aspects - low marginal prices and CO<sub>2</sub> supply costs - play a significant role in the decision on the location of eFuel production units. Average marginal prices are lower in northern Germany, where favorable wind circumstances exist. This tendency is clearly visible when looking at the distribution of eFuel facilities, depicted as the location and capacity of electrolysis units in Fig. 8.

When comparing spatial distributions, it is apparent that in the No-RED scenario a larger share of electrolysis units are installed further away from the German coastline, close to the Polish border and in Saxony-Anhalt. One primary reason is the availability of a direct CO<sub>2</sub> source at these locations, which, without the purchase conditions, proves to be the optimal solution over maximizing nodal wind energy availability.

Expectedly, the inclusion of the geographical correlation condition changes the spatial distribution of electrolysis units. The condition

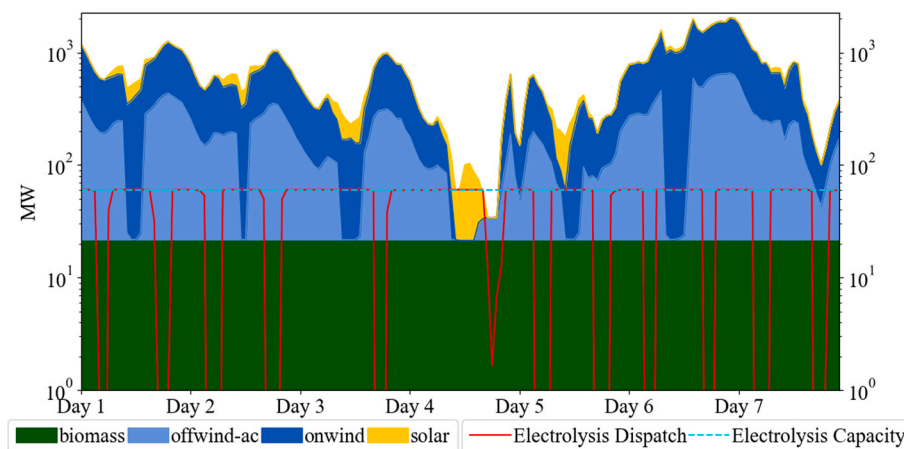


Fig. 5. Electrolysis operation of one exemplary electrolysis unit in 2030 in the No-RED scenario.

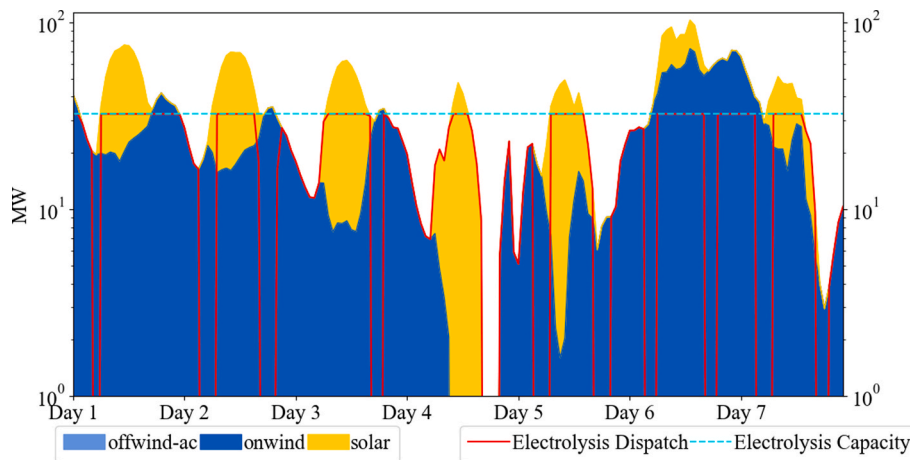


Fig. 6. Electrolysis operation of the largest electrolysis unit in 2030 in the RED scenario.

**Table 4**  
Average utilization of the electrolysis units in the No-RED and RED scenario.

Parameter	No-RED		RED	
Year	2025	2030	2025	2030
Average Utilization [h]	7984	5875	7336	5203

removes the option of installing electrolysis capacity at network nodes without renewable generation, while also limiting viable capacities according to the available wind and solar potential at the same location. Thus, a shift from direct CO<sub>2</sub> sources as the primary driver in location choice towards available renewable potential and high capacity factors can be observed in the results.

6.2. Impact on the energy system

6.2.1. Renewable capacities and distribution

Table 5 shows renewable capacities in GW for each scenario in 2030. Both scenarios with additional eFuels demand unsurprisingly result in increased renewable capacities. The main driver is the increased electricity demand and the necessity to achieve the proper share of renewable energies.

Fig. 9 shows the relative change of wind and solar capacities

compared to the reference scenario. The No-RED and the RED scenario both have higher wind capacities than the reference scenario. The offshore capacities differ only slightly from the reference scenario, but solar and onshore capacities increase in each. Hence, both scenarios result in higher RES capacities, mainly because of the increased electricity demand, but, in the case of the RED scenario, also because the PtL demand needs to be covered fully by RES generation.

It is further visible that the RED scenario will install more solar capacities and less wind onshore capacities. The reason might be the diversification of the electricity supply. Using solar generation might help to close gaps in the wind generation and, therefore, increase the utilization of the constrained electrolysis. This circumstance is visible in Fig. 6. As the electrolysis units are located close to the shore where solar capacity factors are lower, the solar capacities might have to be increased to achieve sufficient solar generation.

Table 6 shows the curtailment of RES in 2030 for the different scenarios. It is observable that the curtailment reduces with the installation of electrolysis units and especially reduces when constraints to increase the correlation between renewable energy generation and electrolysis electricity consumption are implemented. Therefore, the overall flexibility of electrolysis units in combination with hydrogen storage help to integrate renewable energy generation.

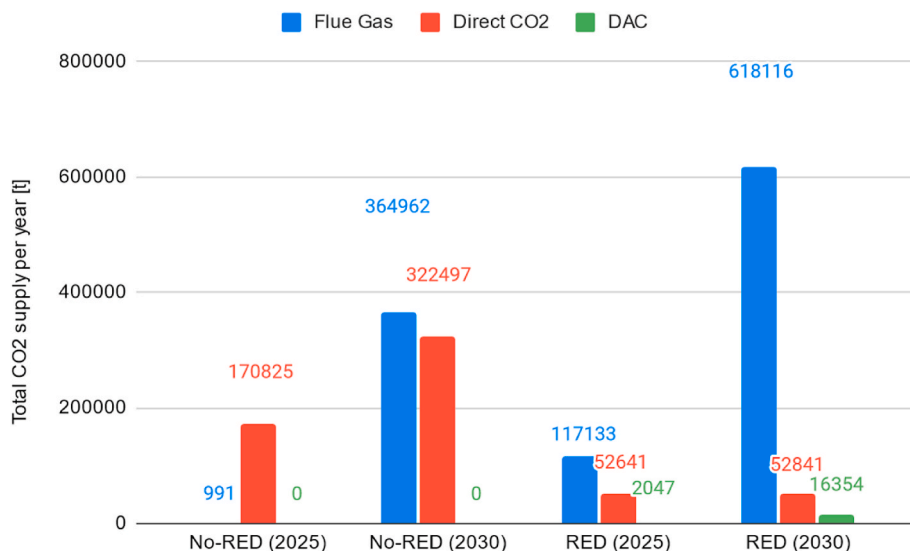


Fig. 7. CO<sub>2</sub> quantity covered by the flue gas route (blue), direct CO<sub>2</sub> route (red) and DAC route (green) in 2025 and 2030 in the No-RED and RED scenarios.

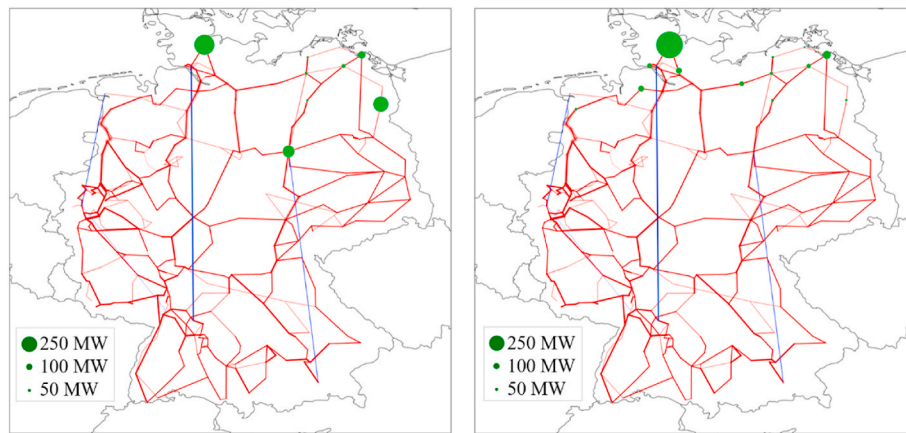


Fig. 8. Transmission lines and electrolysis capacities in 2030 in the No-RED scenario (left) and RED scenario (right).

Table 5

Installed renewable generation capacities in the reference, No-RED and RED scenario.

Scenario	Solar [GW]	Onshore Wind [GW]	Offshore Wind [GW]
Reference	144,580	95,720	13,614
No-RED	146,630	96,540	13,609
RED	147,410	96,210	13,621

6.2.2. CO<sub>2</sub> abatement costs

CO<sub>2</sub> abatement costs give information about the additional costs of energy systems to reduce CO<sub>2</sub> compared to energy systems without these efforts. To calculate CO<sub>2</sub> abatement costs, the total costs of the reference scenario are subtracted from the total costs of the No-RED or RED scenario each. The cost differences are discounted to the year 2020 and divided by the total amount of saved CO<sub>2</sub>. Table 7 shows the CO<sub>2</sub> abatement costs. In the No-RED scenario, CO<sub>2</sub> abatement costs are 429.0 € /t CO<sub>2</sub>. The RED scenario has CO<sub>2</sub> abatement costs of 490.6 € /tCO<sub>2</sub>. While RED II conditions result in additional costs for the energy system, both CO<sub>2</sub> abatement costs differ by 14.3%.

The majority of additional costs in both scenarios stem from the investment in renewable generation, electrolysis, hydrogen storage and CO<sub>2</sub> supply. Looking at the capacities of RES and the different components of the synthesis, it is observable that the constrained purchase in the RED scenario results in higher solar, electrolysis, and storage

capacities, and the utilization of DAC. These additional investments explain the difference between both abatement costs.

Fig. 10 shows the share of the different components on the abatement costs. CO<sub>2</sub> has only a small share, supporting the statement that the decision regarding optimal location is mainly influenced by the available electricity. Both strategies contribute to reduce the investments into the grid, but this reduction is neglectable compared to the additional costs of the energy system from eFuel production.

7. Conclusions & policy implications

In this paper, we presented an approach to investigate the impact of

Table 6

Curtailement of electricity from RES in 2030 for each scenario.

	Reference	No-RED	RED
Curtailement	7.0%	6.9%	6.8%

Table 7

CO<sub>2</sub> abatement costs of the No-RED and RED scenario.

	No-RED	RED
CO <sub>2</sub> abatement costs [€ /t]	429.05	490.58

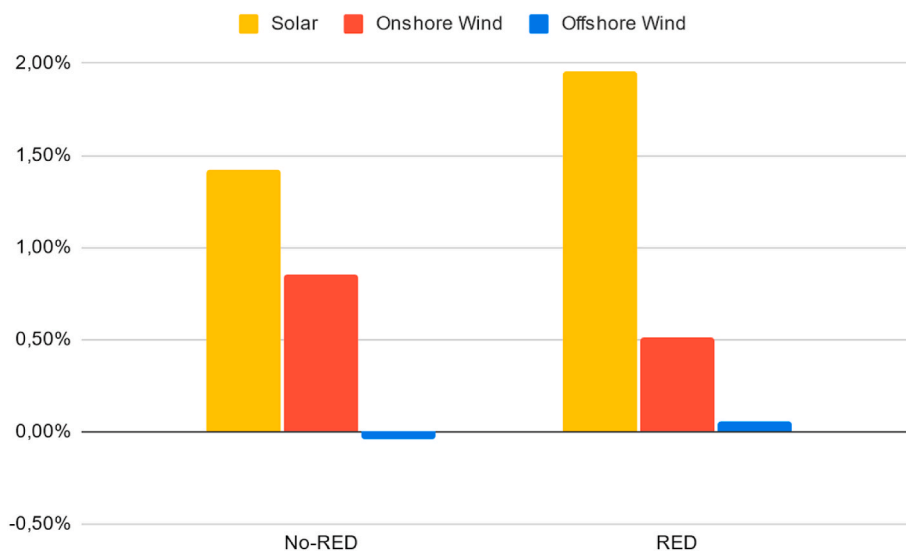
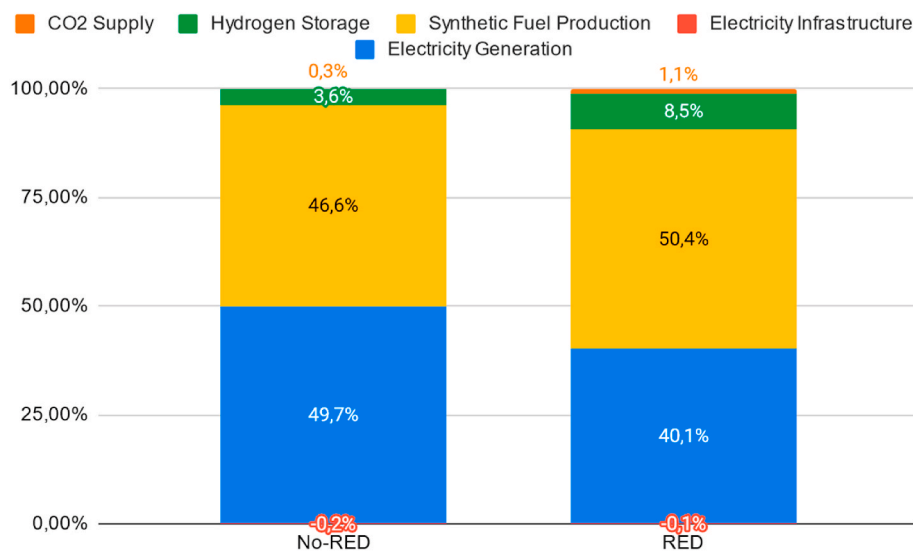


Fig. 9. Changed wind and solar capacities in % compared to the reference scenario.



**Fig. 10.** Share of CO<sub>2</sub> supply costs (orange), hydrogen storage costs (green), eFuel production costs (yellow), electricity infrastructure costs (red) and electricity generation costs (blue) on the CO<sub>2</sub> abatement costs. Due to the high flexibility demand of the electrolysis and the low flexibility of the synthesis units in the RED scenario, hydrogen storage capacities increase and its share on the CO<sub>2</sub> abatement costs rise.

electricity purchase conditions of the Renewable Energy Directive II (RED II) on eFuels production, which is applied to a case study in the German energy system. According to the RED II, three conditions need to be met to classify eFuel as sourced from renewable sources: First, the electricity used to produce the eFuel must stem from renewable sources. Second, the additionality constraint defines that eFuel production should result in additional renewable capacities. Third, the temporal and geographical correlation between renewable electricity generation and electrolysis electricity consumption needs to be met. We used a linear optimization energy system model that accounts for the electricity transmission network as well as CO<sub>2</sub> sources, electrolysis, hydrogen and battery storage, and synthesis. In a second step, additional constraints accounting for the three purchase conditions were added. We compared two scenarios, with and without electricity purchase constraints, which include the objective of producing the quota of 2% aviation fuel in Germany by 2030.

The chosen approach and the case study are subject to a number of limitations. The power-to-liquid process is only investigated at from the system's perspective, and uncertainty remains whether the derived dimensioning and operation conditions are sufficient for economical operation, which might also stem from additional benefits such as balancing energy. As eFuels production technology is still developing, there are several uncertainties with regard to future development. A significant uncertainty is future investment expenditures necessary for electrolysis and DAC units, faster realization of cost reduction potentials could increase economical attractiveness. Furthermore, the uncertainties of the energy system case study itself can be mentioned. Here, the load demand, the transmission grid and several other aspects might develop differently in the long-term than assumed. From the energy system modeling perspective, several uncertainties could affect the results. Compared to conventional kerosene demand, the estimated demand to be fulfilled by electrolysis by 2030 in this work is relatively low. Higher eFuel would have a more emphasized impact on the energy system and will very likely result in a more substantial transformation of the energy system, which might be difficult to achieve by 2030. In addition, the geographical location of the eFuel demand in this work is assumed to be restricted on a national level only. Higher spatial granularity in demand modeling might affect the decision on the optimal location of production facilities. To further improve accuracy in modeling the hydrogen sector of the energy system, the existing approach could be extended to include future hydrogen infrastructure,

such as pipelines, storage facilities, and major demand locations in future work. Furthermore, the input data when using representative data for future energy scenarios depends on the accuracy of the clustering approach and might differ from results using entire time-series data. Finally, the national scope of this work is limited to Germany. In future work, an extension to the central European energy system is desirable to account for the interdependencies between the interconnected systems, especially when modeling the electricity system.

The results show that the electricity purchase conditions have major impacts on dimensioning and operation of Fischer-Tropsch eFuels production. The required capacity of electrolysis increased by 9.05% (2025) and 15.77% (2030), and average electrolysis utilization drops from 5875 h to 5203 h in 2030 (7984 h to 7336 h in 2025) when electricity purchase conditions are applied. The condition of temporal correlation forces the electrolysis to adapt to volatile renewable generation. With electricity purchase conditions, locations with large capacities of newly installed renewable energies are more attractive as the ratio between renewable capacities and electrolysis capacity supports high electrolysis utilization under RED II restrictions. This aspect, along with the additional purchase condition, results in higher solar, offshore wind, and onshore wind capacities. Even with the change in optimal electrolysis location, utilization of electrolysis is lower when purchase conditions are considered. CO<sub>2</sub> takes a minor role regarding placement of power-to-liquid facilities, but increases in importance if electricity purchase is not constrained. In comparison to the CO<sub>2</sub> abatement costs in the No-RED scenario, abatement costs in the RED scenario increased by 14.34%. Conditions for electricity purchase of electrolysis increases investment, especially in solar capacities, as achieving the highest possible electrolysis utilization is the cost-optimal solution. With eFuels production and purchase conditions, the volume of curtailed electricity reduces and lower investments into the electricity grid are necessary. However, the abatement costs show that these positive effects are neglectable when compared to the additional costs from eFuels production, storage, and renewable generation.

Based on the results of this work, the following policy implications can be derived. First, the high CO<sub>2</sub> abatement costs of power-to-liquid applications show that their grid-connected application might be less favorable than alternatives like electric mobility. This circumstance does not necessarily mean that eFuels are less favorable in general. The production within stand-alone power-to-liquid facilities with higher renewable capacity factors might reduce the CO<sub>2</sub> abatement costs

significantly and might be more suitable, especially when the economic maturity of the technology is low. In addition, the increase of the CO<sub>2</sub> abatement costs by only 14.34% more than the scenario without electricity purchase criteria shows that the implementation of electricity purchase criteria might be a suitable approach from the energy system planner's perspective. However, the question arises if the increased investment into the power-to-liquid facility when applying electricity purchase conditions result in economic feasibility of the eFuel production. Subsidies to support producers, especially in the early stage of the upcoming green hydrogen industry, might be necessary. Altogether, it might be an efficient solution to locate early electrolysis capacities close to the renewable generators and use electrolysis as a flexible supply in later stages of the development of a hydrogen-based system where lower investment allows economical operation with lower utilization. Furthermore, the approach to dimension the electrolysis at lower capacities than the corresponding RES capacities in combination with the diversification of electricity supply by using both, wind and solar capacities, allow high utilization of electrolysis even with grid-connected systems. The advantage of this approach is that residual energy between renewable generation and electrolysis demand can be fed-in into

the electricity grid and, therefore, be sold at spot markets to create an additional revenue stream.

### CRediT authorship contribution statement

**Uwe Langenmayr:** Conceptualization, Data curation, Formal analysis, Methodology, Software, Validation, Visualization, Writing – original draft, Writing – review & editing. **Manuel Ruppert:** Conceptualization, Data curation, Formal analysis, Methodology, Validation, Writing – original draft, Writing – review & editing.

### Declaration of competing interest

The authors declare that they have no known competing financial interests or personal relationships that could have appeared to influence the work reported in this paper.

### Data availability

The data and code is already open source available (see references).

## A. Appendix

### A.1 Economic assumptions of CO<sub>2</sub> scrubber unit, synthesis and hydrogen storage.

Component	CAPEX	Fixed O&M	Variable O&M	Lifetime	Reference
CO <sub>2</sub> scrubber	130911 [€ /t *h]	9 [% of investment]	0	20 [years]	<a href="#">Heinzmann et al. (2021)</a>
Synthesis	1371624 [€ /MW Hydrogen]	9 [% of investment]	14.49 [€ /MW Hydrogen]	20 [years]	<a href="#">Heinzmann et al. (2021)</a>
Hydrogen storage	490 [€ /kg]	1 [% of investment]	0	20 [years]	<a href="#">Gorre et al. (2020)</a>

### A.2 Economic assumptions of electrolysis and DAC units

	2020	2025	2030	Reference
<b>CAPEX</b>				
Electrolysis [€ /MW]	1000	873	810	<a href="#">Heinzmann et al. (2021)</a>
DAC [€ /t <sub>CO2</sub> * a]	730	540	340	<a href="#">Fasihi et al. (2019)</a>
<b>Lifetime [Years]</b>				
Electrolysis	20	20	20	<a href="#">Heinzmann et al. (2021)</a>
DAC	20	20	20	<a href="#">Fasihi et al. (2019)</a>
<b>Fixed O&amp;M [% of investment]</b>				
Electrolysis	5	5	5	<a href="#">Heinzmann et al. (2021)</a>
DAC	4	4	4	<a href="#">Fasihi et al. (2019)</a>
<b>Variable O&amp;M</b>				
Electrolysis [€ /MW Electricity]	0.005	0.005	0.005	<a href="#">Heinzmann et al. (2021)</a>
DAC	0	0	0	<a href="#">Fasihi et al. (2019)</a>

### A.3 Technical assumptions of the eFuel production route

Component	Unit	2020	2025	2030	Reference
Electrolysis	Efficiency	61.2	61.6	62	<a href="#">Heinzmann et al. (2021)</a>
CO <sub>2</sub> scrubber	t CO <sub>2</sub> /t Flue gas	0.286	0.286	0.286	<a href="#">Heinzmann et al. (2021)</a>
DAC	t CO <sub>2</sub> /MW Electricity	4	4	4	<a href="#">Fasihi et al. (2019)</a>
Synthesis	MW Syncrude /MW Hydrogen	60.6	60.6	60.6	<a href="#">Heinzmann et al. (2021)</a>
Synthesis	t CO <sub>2</sub> /MWh Fuel	0.173	0.173	0.173	<a href="#">Heinzmann et al. (2021)</a>

### A.4 Energy system related assumptions. Other relevant assumptions are taken from [Hörsch et al. \(2018a\)](#).

Component	Parameter	Unit	2020	2025	2030	Reference
Wind Offshore	CAPEX	€/kW	3467	3052	2637	Keles and Yilmaz (2020)
Wind Offshore	Fixed O&M	€/kW*a	113	99.5	86	
Wind Offshore	Variable O&M	€/kWh	0.5	0.5	0.5	
Wind Onshore	CAPEX	€/kW	1619	1489	1243	
Wind Onshore	Fixed O&M	€/kW*a	32	29.5	27	
Wind Onshore	Variable O&M	€/kWh	0.5	0.5	0.5	
Photovoltaic	CAPEX	€/kW	649	610	570	
Photovoltaic	Fixed O&M	€/kW*a	1.6	1.5	1.4	
Photovoltaic	Variable O&M	€/kWh	0.1	0.1	0.1	
Biomass	CAPEX	€/kW	5012	4823	4634	
Biomass	Fixed O&M	€/kW*a	136	133.5	131	
Biomass	Variable O&M	€/kWh	0	0	0	

## References

- Arbeitsgemeinschaft Energiebilanzen e.V., 2021. 1 Auswertungstabellen zur Energiebilanz Deutschland. Daten für die Jahre von 1990 bis 2020. [https://ag-energiebilanzen.de/wp-content/uploads/2020/09/awt\\_2020\\_d.pdf](https://ag-energiebilanzen.de/wp-content/uploads/2020/09/awt_2020_d.pdf) checked on 3/23/2022.
- Ashfaq, Asad, Kamali, Zulqarnain Haider, Agha, Mujtaba Hassan, Arshid, Hirra, 2017. Heat coupling of the pan-European vs. regional electrical grid with excess renewable energy. *Energy* 122, 363–377. <https://doi.org/10.1016/j.energy.2017.01.084>.
- Blanco, Herib, Nijs, Wouter, Ruf, Johannes, Faaij, André, 2018a. Potential for hydrogen and Power-to-Liquid in a low-carbon EU energy system using cost optimization. *Appl. Energy* 232, 617–639. <https://doi.org/10.1016/j.apenergy.2018.09.216>.
- Blanco, Herib, Nijs, Wouter, Ruf, Johannes, Faaij, André, 2018b. Potential of power-to-methane in the EU energy transition to a low carbon system using cost optimization. *Appl. Energy* 232, 323–340. <https://doi.org/10.1016/j.apenergy.2018.08.027>.
- Bogdanov, Dmitrii, Gulagi, Ashish, Fasihi, Mahdi, Breyer, Christian, 2021. Full energy sector transition towards 100% renewable energy supply: integrating power, heat, transport and industry sectors including desalination. *Appl. Energy* 283, 116273. <https://doi.org/10.1016/j.apenergy.2020.116273>.
- Brand, Christian, Tran, Martino, Anable, Jillian, 2012. The UK transport carbon model: an integrated life cycle approach to explore low carbon futures. *Energy Pol.* 41, 107–124. <https://doi.org/10.1016/j.enpol.2010.08.019>.
- Brown, Tom, Hörsch, Jonas, Schlachtberger, David, 2018. PyPSA: Python for power system analysis. *J. Open Res. Software* 6. <https://doi.org/10.5334/jors.188>. Article 4.
- Bundesamt für Justiz (8/14/2020): Gesetz zur Reduzierung und zur Beendigung der Kohleverbrennung\* (Kohleverbrennungsbeendigungsgesetz - KVBG). KVBG. Available online at: <https://www.gesetze-im-internet.de/kvbgb/BjNR181810020.html>.
- Bundesnetzagentur, 2021. Marktstammdatenregister. <https://www.marktstammdatenregister.de/MaStR/Datendownload> checked on 12/14/2021.
- Bundesverband der deutschen Bioethanolwirtschaft e.V., 2021. Bioethanolproduktion seit 2005. <https://www.bdbe.de/biokraftstoff-bioethanol/zellulose-ethanol> checked on 12/14/2021.
- Capros, Pantelis, Zazias, Georgios, Evangelopoulou, Stavroula, Kannavou, Maria, Fotiou, Theofano, Siskos, Pelopidas, et al., 2019. Energy-system modelling of the EU strategy towards climate-neutrality. *Energy Pol.* 134 (8), 110960 <https://doi.org/10.1016/j.enpol.2019.110960>.
- Chiaromonti, David, Goumas, Theodor, 2019. Impacts on industrial-scale market deployment of advanced biofuels and recycled carbon fuels from the EU Renewable Energy Directive II. *Appl. Energy* 251 (August), 113351. <https://doi.org/10.1016/j.apenergy.2019.113351>.
- Dahal, Karna, Juhola, Sirkku, Niemelä, Jari, 2018. The role of renewable energy policies for carbon neutrality in Helsinki Metropolitan area. *Sustain. Cities Soc.* 40 (3), 222–232. <https://doi.org/10.1016/j.scs.2018.04.015>.
- Deutsche Emissionshandlungsstelle, 2021. Treibhausgasemissionen 2020. Emissionshandlungspflichtige stationäre Anlagen und Luftverkehr in Deutschland (VET-Bericht 2020). [https://www.dehst.de/SharedDocs/downloads/DE/publikationen/VET-Bericht-2020.pdf;jsessionid=69E65A7F02764A76F48CD2D59B07806A.1\\_cid331?\\_blob=publicationFile&v=4](https://www.dehst.de/SharedDocs/downloads/DE/publikationen/VET-Bericht-2020.pdf;jsessionid=69E65A7F02764A76F48CD2D59B07806A.1_cid331?_blob=publicationFile&v=4) checked on 12/14/2021.
- Deutsche Energie-Agentur, 2021. Biogas Einspeiseatlas Deutschland. <https://www.biogaspartner.de/einspeiseatlas/> checked on 12/14/2021.
- European Union, 2022. COMMISSION DELEGATED REGULATION (EU) .../... of XXX supplementing Directive (EU) 2018/2001 of the European Parliament and of the Council by establishing a Union methodology setting out detailed rules for the production of renewable liquid and gaseous transport fuels of non-biological origin 2022 (L 328/82). <https://ec.europa.eu/info/law/better-regulation/have-your-say/initiatives/7046068-Production-of-renewable-transport-fuels-share-of-renewable-electricity-requirements-en> checked on 6/23/2022.
- European Union (4/25/2023): Fit for 55: Parliament and Council reach deal on greener aviation fuels. Available online at: <https://www.europarl.europa.eu/news/en/press-room/20230424IPR82023/fit-for-55-parliament-and-council-reach-deal-on-greener-aviation-fuels>, checked on 8/22/2023..
- Fasihi, Mahdi, Efimova, Olga, Breyer, Christian, 2019. Techno-economic assessment of CO2 direct air capture plants. *J. Clean. Prod.* 224 (3), 957–980. <https://doi.org/10.1016/j.jclepro.2019.03.086>.
- Available online at. In: Fischechick, Manfred, Görner, Klaus, Thomeczek, Margit (Eds.), 2015. CO2: Abtrennung, Speicherung, Nutzung. Ganzheitliche Bewertung im Bereich von Energiewirtschaft und Industrie. Springer Berlin Heidelberg, Berlin, Heidelberg <http://nbn-resolving.org/urn:nbn:de:bsz:31-epflicht-1574888>.
- Frysztacki, Martha Maria, Hörsch, Jonas, Hagenmeyer, Veit, Brown, Tom, 2021. The strong effect of network resolution on electricity system models with high shares of wind and solar. *Appl. Energy* 291, 116726. <https://doi.org/10.1016/j.apenergy.2021.116726>.
- Gea-Bermúdez, Juan, Jensen, Ida Græsted, Münster, Marie, Koivisto, Matti, Kirkerud, Jon Gustav, Chen, Yi-kuang, Ravn, Hans, 2021. The role of sector coupling in the green transition: a least-cost energy system development in Northern-central Europe towards 2050. *Appl. Energy* 289, 116685. <https://doi.org/10.1016/j.apenergy.2021.116685>.
- Gils, Hans Christian, Gardian, Hedda, Schmutz, Jens, 2021. Interaction of hydrogen infrastructures with other sector coupling options towards a zero-emission energy system in Germany. *Renew. Energy* 180, 140–156. <https://doi.org/10.1016/j.renene.2021.08.016>.
- Gorre, Jachin, Ruoss, Fabian, Karjunen, Hannu, Schaffert, Johannes, Tynjälä, Tero, 2020. Cost benefits of optimizing hydrogen storage and methanation capacities for Power-to-Gas plants in dynamic operation. *Appl. Energy* 257 (1–2), 113967. <https://doi.org/10.1016/j.apenergy.2019.113967>.
- Gudmundsson, Oddgeir, Thorsen, Jan Eric, Brand, Marek, 2018. The role of district heating in coupling of the future renewable energy sectors. *Energy Proc.* 149, 445–454. <https://doi.org/10.1016/j.egypro.2018.08.209>.
- Hanley, Emma S., Deane, J.P., Gallachóir, B.Ó.P., 2018. The role of hydrogen in low carbon energy futures—A review of existing perspectives. *Renew. Sustain. Energy Rev.* 82, 3027–3045. <https://doi.org/10.1016/j.rser.2017.10.034>.
- Hansen, Kenneth, Breyer, Christian, Lund, Henrik, 2019. Status and perspectives on 100% renewable energy systems. *Energy* 175, 471–480. <https://doi.org/10.1016/j.energy.2019.03.092>.
- Heinisch, Verena, Göransson, Lisa, Erlandsson, Rasmus, Hodel, Henrik, Johnsson, Filip, Odenberger, Mikael, 2021. Smart electric vehicle charging strategies for sectoral coupling in a city energy system. *Appl. Energy* 288, 116640. <https://doi.org/10.1016/j.apenergy.2021.116640>.
- Heinzmann, Paul, Glöser-Chahoud, Simon, Dahmen, Nicolaus, Langenmayr, Uwe, Schultmann, Frank, 2021. Techno-ökonomische Bewertung der Produktion regenerativer synthetischer Kraftstoffe.
- Helgeson, Broghan, Peter, Jakob, 2020. The role of electricity in decarbonizing European road transport – development and assessment of an integrated multi-sectoral model. *Appl. Energy* 262, 114365. <https://doi.org/10.1016/j.apenergy.2019.114365>.
- Hörsch, Jonas, Hofmann, Fabian, Schlachtberger, David, Brown, Tom, 2018a. PyPSA-Eur: an open optimisation model of the European transmission system. *Energy Strategy Res.* 22, 207–215. <https://doi.org/10.1016/j.esr.2018.08.012>.
- Hörsch, Jonas, Ronellenfitsch, Henrik, Witthaut, Dirk, Brown, Tom, 2018b. Linear optimal power flow using cycle flows. *Elec. Power Syst. Res.* 158, 126–135. <https://doi.org/10.1016/j.epsr.2017.12.034>.
- Jimenez-Navarro, Juan-Pablo, Kavvadias, Konstantinos, Filippidou, Faidra, Pavičević, Matija, Quoilin, Sylvain, 2020. Coupling the heating and power sectors: the role of centralised combined heat and power plants and district heat in a European decarbonised power system. *Appl. Energy* 270, 115134. <https://doi.org/10.1016/j.apenergy.2020.115134>.
- Keles, Dogan, Yilmaz, Hasan Ümitcan, 2020. Decarbonisation through coal phase-out in Germany and Europe — impact on Emissions, electricity prices and power production. *Energy Pol.* 141 (2), 111472 <https://doi.org/10.1016/j.enpol.2020.111472>.
- Kiviluoma, Juha, Meibom, Peter, 2011. Methodology for modelling plug-in electric vehicles in the power system and cost estimates for a system with either smart or dumb electric vehicles. *Energy* 36 (3), 1758–1767. <https://doi.org/10.1016/j.energy.2010.12.053>.
- Luderer, Gunnar, Kost, Christoph, Dominika, 2021. Deutschland auf dem Weg zur Klimaneutralität 2045 - Szenarien und Pfade im Modellvergleich. Potsdam Institute for Climate Impact Research.

- Meibom, Peter, Kiviluoma, Juha, Barth, Rüdiger, Brand, Heike, Weber, Christoph, Larsen, Helge V., 2007. Value of electric heat boilers and heat pumps for wind power integration. *Wind Energy* 10 (4), 321–337. <https://doi.org/10.1002/we.224>.
- Meisel, Kathleen, Braune, Maria, Gröngroft, Arne, Majer, Stefan, Müller-Langer, Franziska, Naumann, Karin, Oehmichen, Katja, 2015. Technische und methodische Grundlagen der THG-Bilanzierung von Bioethanol. Handreichung. Leipzig, Dresden: DBFZ Deutsches Biomasseforschungszentrum gemeinnützige GmbH; Sächsische Landesbibliothek – staats- und Universitätsbibliothek Dresden. Available online at: <https://nbn-resolving.de/urn:nbn:de:bsz:14-qucosa2-357054>.
- Mesfun, Sennai, Sanchez, Daniel L., Leduc, Sylvain, Wetterlund, Elisabeth, Lundgren, Joakim, Biberacher, Markus, Kraxner, Florian, 2017. Power-to-gas and power-to-liquid for managing renewable electricity intermittency in the Alpine Region. *Renew. Energy* 107, 361–372. <https://doi.org/10.1016/j.renene.2017.02.020>.
- Nevens, Frank, Roorda, Chris, 2014. A climate of change: a transition approach for climate neutrality in the city of Ghent (Belgium). *Sustain. Cities Soc.* 10, 112–121. <https://doi.org/10.1016/j.scs.2013.06.001>.
- Osorio-Aravena, Juan Carlos, Aghahosseini, Arman, Bogdanov, Dmitrii, Caldera, Upeksha, Ghorbani, Narges, Mensah, Theophilus Nii Odai, et al., 2021. The impact of renewable energy and sector coupling on the pathway towards a sustainable energy system in Chile. *Renew. Sustain. Energy Rev.* 151, 111557 <https://doi.org/10.1016/j.rser.2021.111557>.
- Pavičević, Matija, Mangipinto, Andrea, Nijs, Wouter, Lombardi, Francesco, Kavvadias, Konstantinos, Navarro, Jiménez, Juan Pablo, et al., 2020. The potential of sector coupling in future European energy systems: soft linking between the Dispa-SET and JRC-EU-TIMES models. *Appl. Energy* 267, 115100. <https://doi.org/10.1016/j.apenergy.2020.115100>.
- Pensini, Alessandro, Rasmussen, Claus N., Kempton, Willett, 2014. Economic analysis of using excess renewable electricity to displace heating fuels. *Appl. Energy* 131, 530–543. <https://doi.org/10.1016/j.apenergy.2014.04.111>.
- Plötz, Patrick, Gnann, Till, Jochem, Patrick, Yilmaz, Hasan Ümitcan, Kaschub, Thomas, 2019. Impact of electric trucks powered by overhead lines on the European electricity system and CO2 emissions. *Energy Pol.* 130, 32–40. <https://doi.org/10.1016/j.enpol.2019.03.042>.
- Quarton, Christopher J., Samsatli, Sheila, 2020. The value of hydrogen and carbon capture, storage and utilisation in decarbonising energy: insights from integrated value chain optimisation. *Appl. Energy* 257 (5), 113936. <https://doi.org/10.1016/j.apenergy.2019.113936>.
- Ramsebnner, Jasmine, Haas, Reinhard, Ajanovic, Amela, Wietschel, Martin, 2021. The sector coupling concept: a critical review. *WIREs Energy Environ.* 10 (4), 1. <https://doi.org/10.1002/wene.396>.
- Ruhnau, Oliver, Schiele, Johanna, 2022. Flexible green hydrogen: economic benefits without increasing power sector emissions. Available online at: In: ZBW - Leibniz Information Centre for Economics, Kiel, Hamburg <http://hdl.handle.net/10419/258999>, checked on 6/23/2022.
- Scheelhaase, Janina, Maertens, Sven, Grimme, Wolfgang, 2019. Synthetic fuels in aviation – current barriers and potential political measures. *Transport. Res. Procedia* 43, 21–30. <https://doi.org/10.1016/j.trpro.2019.12.015>.
- Schill, Wolf-Peter, Gerbaulet, Clemens, 2015. Power system impacts of electric vehicles in Germany: charging with coal or renewables? *Appl. Energy* 156, 185–196. <https://doi.org/10.1016/j.apenergy.2015.07.012>.
- Schlund, David, Theile, Philipp, 2022. Simultaneity of green energy and hydrogen production: analysing the dispatch of a grid-connected electrolyser. *Energy Pol.* 166, 113008 <https://doi.org/10.1016/j.enpol.2022.113008>.
- Seljom, Pernille, Rosenberg, Eva, 2018. A scandinavian transition towards a carbon-neutral energy system. In: George, Giannakidis (Ed.), *Limiting Global Warming to Well below 2 °C*, Vol. 64. With Assistance of Kenneth Karlsson, Maryse Labriet, Brian Ó. Gallachóir. Springer (Lecture Notes in Energy Ser., v. 64), Cham, pp. 105–121.
- Sensfuß, Frank, Lux, Benjamin, Bernath, Christiane, Kiefer, Christoph, Pfluger, Benjamin, Kleinschmitt, Chris, 2021. Langfristszenarien für die Transformation des Energiesystems in Deutschland. *Treibhausgasneutrale Hauptszenarien Modul Energieangebot*. Edited by Bundesministerium für Wirtschaft und Energie (BMWi). Consentec GmbH; Fraunhofer-Institut für System- und Innovationsforschung ISI; ifeu – Institut für Energie- und Umweltforschung Heidelberg. Technische Universität Berlin.
- Siegemund, Stefan, Trommler, Marcus, Kolb, Ole, Zinnecker, Valentin, 2017. «E-FUELS» STUDY. The potential of electricity-based fuels for low-emission transport in the EU. An expertise by LBST and dena. Edited by Deutsche Energie-Agentur GmbH (dena). Deutsche Energie-Agentur GmbH; Ludwig-Bölkow-Systemtechnik GmbH. Berlin. [https://www.dena.de/fileadmin/dena/Dokumente/Pdf/9219\\_E-FUELS-STUDY\\_The\\_potential\\_of\\_electricity\\_based\\_fuels\\_for\\_low\\_emission\\_transport\\_in\\_the\\_EU.pdf](https://www.dena.de/fileadmin/dena/Dokumente/Pdf/9219_E-FUELS-STUDY_The_potential_of_electricity_based_fuels_for_low_emission_transport_in_the_EU.pdf) checked on 3/22/2022.
- Wang, Huan, Chen, Wenying, Shi, Jingcheng, 2018. Low carbon transition of global building sector under 2- and 1.5-degree targets. *Appl. Energy* 222 (2), 148–157. <https://doi.org/10.1016/j.apenergy.2018.03.090>.
- Yilmaz, Hasan Ümitcan, Fouché, Edouard, Dengiz, Thomas, Krauß, Lucas, Keles, Dogan, Fichtner, Wolf, 2019. Reducing energy time series for energy system models via self-organizing maps. *IT Inf. Technol.* 61 (2-3), 125–133. <https://doi.org/10.1515/itit-2019-0025>.